

2.1.3.2 Kinetic Isotope Effects

Large hydrogen isotope fractionations occur during the conversion of hydrogen from water to organic matter. The magnitude of H isotope fractionations is generally controlled by the biochemical pathways used. Although details of this complex process are still unknown, there is discussion about the quantitative role of kinetic and equilibrium isotope fractionations. Tremendous progress has been achieved through the introduction of the compound specific hydrogen isotope analysis (Sessions et al. 1999; Sauer et al. 2001; Schimmelmann et al. 2006), which allows the δD analysis of individual biochemical compound. Further details are discussed in Sect. 3.10.1.2.

2.1.3.3 Other Fractionation Effects

In salt solutions, isotopic fractionations can occur between water in the “hydration sphere” and free water (Truesdell 1974). The effects of dissolved salts on hydrogen isotope activity ratios in salt solutions can be qualitatively interpreted in terms of interactions between ions and water molecules, which appear to be primarily related to their charge and radius. Hydrogen isotope activity ratios of all salt solutions studied so far are appreciably higher than H-isotope composition ratios. As shown by Horita et al. (1993), the D/H ratio of water vapor in isotope equilibrium with a solution increases as salt is added to the solution. Magnitudes of the hydrogen isotope effects are in the order $\text{CaCl}_2 > \text{MgCl}_2 > \text{MgSO}_4 > \text{KCl} \sim \text{NaCl} > \text{NaSO}_4$ at the same molality.

Isotope effects of this kind are relevant for an understanding of the isotope composition of clay minerals and absorption of water on mineral surfaces. The tendency for clays and shales to act as semipermeable membranes is well known. This effect is also known as “ultrafiltration”. Coplen and Hanshaw (1973) postulated that hydrogen isotope fractionations may occur during ultrafiltration in such a way that the residual water is enriched in deuterium due to its preferential adsorption on the clay minerals and its lower diffusivity.

2.2 Lithium

Lithium has two stable isotopes with the following abundances (Rosman and Taylor 1998):

^6Li 7.59%

^7Li 92.41%

Lithium is one of the rare elements where the lighter isotope is less abundant than the heavier one. In order to be consistent with the other isotope systems lithium isotope ratios are reported as $\delta^7\text{Li}$ -values.

The large mass difference relative to the mass of the element between ^6Li and ^7Li of about 16% is a favorable condition for their fractionation in nature. Taylor and Urey (1938) found a change of 25% in the Li-isotope ratio when Li-solutions percolate through a zeolite column. Thus, fractionation of Li-isotopes might be expected in geochemical settings in which cation exchange processes are involved.

Early workers had to struggle with serious lithium fractionation effects during mass spectrometric analysis. Today most workers use the multicollector sector ICP-MS technique first described by Tomascak et al. (1999). Improvements of the analytical techniques in recent years have lead to an accuracy better than 0.3‰. Unfortunately, there are no internationally accepted Li isotope values for rocks or waters. James and Palmer (2000) have determined nine international rock standards ranging from basalt to shale relative to the so-called NIST L-SVEC standard.

i) Characteristic features of Li isotope geochemistry

Lithium isotope geochemistry is characterized by a difference close to 30‰ between ocean water ($\delta^7\text{Li} + 31\text{‰}$) and bulk silicate earth with a $\delta^7\text{Li}$ value of 3.2‰ (Seitz et al. 2007). In this respect lithium isotope geochemistry is very similar to that of boron (see p. 45). The isotopic difference between the mantle and the ocean can be used as a powerful tracer to constrain water/rock interactions (Tomaszak 2004). Figure 2.6 gives an overview of Li-isotope variations in major geological reservoirs.

During weathering ^7Li is preferentially mobilized, whereas ^6Li is enriched in the weathering residue. Rudnick et al. (2004) have demonstrated that Li isotope fractionation correlates directly with the degree of weathering and that very light $\delta^7\text{Li}$ of -20‰ can be produced in soils. Thus, very effective Li-isotope fractionation processes are operative in the sedimentary environment. By analyzing major rivers, Huh et al. (1998) observed a large variation in $\delta^7\text{Li}$ in river waters with the suspended load being systematically lighter than the dissolved load.

Mantle-derived basalts, on the other hand, have a relatively uniform composition with $\delta^7\text{Li}$ values of $4 \pm 2\text{‰}$ (Tomaszak 2004; Elliott et al. 2004). The continental crust generally has a lighter Li isotope composition than the upper mantle from which it was derived (Teng et al. 2004). Considering the small Li isotope fractionation at high temperature igneous differentiation processes (Tomaszak 2004), pristine

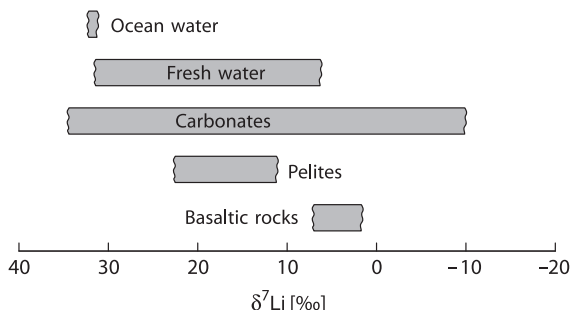


Fig. 2.6 Lithium isotope variations in major geological reservoirs

continental crust should not be too different in Li isotope composition from the mantle. Because this is not the case, the isotopically light crust must have been modified by secondary processes, such as weathering, hydrothermal alteration and prograde metamorphism (Teng et al. 2007).

Given the homogeneity of basaltic rocks, it is surprising that peridotites have a wide range in $\delta^7\text{Li}$ values from values as low as -17‰ (Nishio et al. 2004) to values as high as $+10\text{‰}$ (Brooker et al. 2004). This unexpected finding can be explained by diffusion processes that affect mantle minerals during melt migration (Parkinson et al. 2007). The latter authors have demonstrated that ^6Li diffuses 3% faster than ^7Li in silicate minerals consistent with diffusion experiments by Richter et al. (2003). Thus diffusion at magmatic temperatures is a very effective mechanism for generating large variations in $^7\text{Li}/^6\text{Li}$ ratios (Lundstrom et al. 2005; Teng et al. 2006; Rudnick and Ionov 2007). Although diffusion profiles will relax with time the existence of sharp $\delta^7\text{Li}$ Li-profiles suggest diffusional Li isotope fractionation over short timescales (days to a few months) and therefore diffusion profiles in mantle minerals may be used as geospeedometers (Parkinson et al. 2007). At the same time diffusion may obliterate primary mantle signatures.

During fluid–rock interaction, Li as a fluid-mobile element will enrich in aqueous fluids. It might therefore be expected that $\delta^7\text{Li}$ enriched seawater incorporated into altered oceanic crust should be removed during subduction zone metamorphism. Continuous dehydration of pelagic sediments and altered oceanic crust results in ^7Li -depleted rocks and in ^7Li enriched fluids. A subducting slab therefore should introduce large amounts of ^7Li into the mantle wedge. To quantitatively understand this process Li isotope fractionation factors between minerals and coexisting fluids must be known. First attempts have been undertaken by Wunder et al. (2006, 2007) by determining experimentally the Li isotope fractionations between pyroxene, mica, staurolite and Cl^- and OH^- bearing fluids. These authors showed that ^7Li is preferentially partitioned into the fluid.

Because Li isotopes may be used as a tracer to identify the existence of recycled material in the mantle, systematic studies of arc lavas have been undertaken (Moriguti and Nakamura 1998; Tomascak et al. 2000; Leeman et al. 2004 and others). However, most arc lavas have $\delta^7\text{Li}$ values that are indistinguishable from those of MORB. Thus Li seems to be decoupled from other fluid mobile elements, because Li can partition into Mg-silicates (pyroxene, olivine) in the mantle (Tomascak et al. 2002).

Lithium is a conservative element in the ocean with a residence time of about one million year. Its isotope composition is maintained by inputs of dissolved Li from rivers (average $\delta^7\text{Li} + 23\text{‰}$, Huh et al. 1998) and high-temperature hydrothermal fluids at ocean ridges at one hand and low temperature removal of Li into oceanic basalts and marine sediments at the other. Any variance in these sources and sinks thus should cause secular variations in the isotope composition of oceanic Li. And indeed in a first attempt Hoefs and Sywall (1997) interpreted Li isotope variations in well preserved carbonate shells as indicating secular variations of the oceanic Li-cycle.

2.3 Boron

Boron has two stable isotopes with the following abundances (Rosman and Taylor 1998).

^{10}B 19.9%

^{11}B 80.1%

The large mass difference between ^{10}B and ^{11}B and large chemical isotope effects between different species (Bigeleisen 1965) make boron a very promising element to study for isotope variations. The utility of boron isotopes as a geochemical tracer stems from the high mobility of boron during high- and low-temperature fluid-related processes, showing a strong affinity for any vapor phases present.

The lowest observed $\delta^{11}\text{B}$ -values of around -30‰ are for certain tourmalines (Chaussidon and Albarede 1992) and some non-marine evaporite sequences (Swihart et al. 1986), whereas the most enriched ^{11}B -reservoir is given by brines from Australia and Israel (Dead Sea) which have $\delta^{11}\text{B}$ -values of up to 60‰ (Vengosh et al. 1991a, b). A very characteristic feature of boron geochemistry is the isotopic composition of ocean water with a constant $\delta^{11}\text{B}$ -value of 39.5‰ (Spivack and Edmond 1987), which is about 50‰ heavier than average continental crust value of $-10 \pm 2\text{‰}$ (Chaussidon and Albarede 1992). Isotope variations of boron in some geological reservoirs are shown in Fig. 2.7.

Methods

In recent years solid source mass-spectrometry has provided an effective means for B-isotope analysis. Two different methods have been developed, which have been summarized by Swihart (1996). The first was a positive thermal ionization technique using Na_2BO_2^+ ions initially developed by McMullen et al. (1961). Subsequently, Spivack and Edmond (1986) modified this technique by using Cs_2BO_2^+

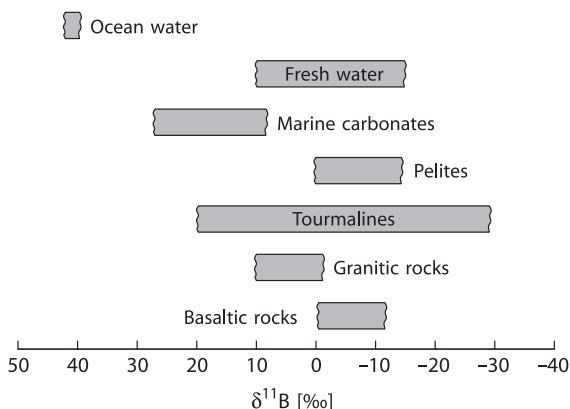


Fig. 2.7 Boron isotope variations in some geologically important reservoirs

ions (measurement of the masses 308 and 309). The substitution of ^{133}Cs for ^{23}Na increases the molecular mass and reduces the relative mass difference of its isotopic species, which limits the thermally induced mass dependent isotopic fractionation. This latter method has a precision of about $\pm 0.25\%$, which is better by a factor of 10 than the Na_2BO_2^+ method. Another method has been used by Chaussidon and Albarede (1992), who performed boron isotope determinations with an ion-microprobe having an analytical uncertainty of about $\pm 2\%$. Recently, Lecuyer et al. (2002) described the use of MC-ICP-MS for B isotopic measurements of waters, carbonates, phosphates and silicates with an external reproducibility of $\pm 0.3\%$.

As analytical techniques have been consistently improved in recent years, the number of boron isotope studies has increased rapidly. Reviews have been given by Barth (1993) and by Palmer and Swihart (1996). The total boron isotope variation documented to date is about 90‰. $\delta^{11}\text{B}$ -values are generally given relative NBS boric acid SRM 951, which is prepared from a Searles Lake borax. This standard has a $^{11}\text{B}/^{10}\text{B}$ ratio of 4.04558 (Palmer and Slack 1989).

pH dependence of isotope fractionations

Boron is generally bound to oxygen or hydroxyl groups in either triangular (e.g., BO_3) or tetrahedral (e.g., $\text{B}(\text{OH})_4^-$) coordination. The dominant isotope fractionation process occurs in aqueous systems via an equilibrium exchange process between boric acid ($\text{B}(\text{OH})_3$) and coexisting borate anion ($\text{B}(\text{OH})_4^-$). At low pH-values trigonal $\text{B}(\text{OH})_3$ predominates, at high pH-values tetrahedral $\text{B}(\text{OH})_4^-$ is the primary anion. The pH-dependence of the two boron species and their related isotope fractionation is shown in Fig. 2.8 (after Hemming and Hanson 1992). The pH dependence has been used reconstructing past ocean pH-values by measuring the boron isotope composition of carbonates e.g. foraminifera. This relies on the fact that mainly the charged species $\text{B}(\text{OH})_4^-$ is incorporated into carbonate minerals with small to insignificant fractionations (Hemming and Hanson 1992; Sanyal et al. 2000).

Because of the inability to quantitatively separate the two species in solution, a theoretically calculated fractionation factor of about 1.0194 at 25°C has been widely used for pH estimates (Kakihana et al. 1977). As recently shown by Zeebe (2005) and Klochko et al. (2006) the equilibrium fractionation factor appears to be significantly larger than the theoretical value of Kakihana et al. (1977) used in paleo-pH studies. Klochko et al. (2006), for instance, reported a fractionation factor of 1.0272.

This approach has been not only used to directly estimate the ocean pH from $\delta^{11}\text{B}$ of foraminifera but to estimate from the pH the past atmospheric CO_2 concentrations (i.e. Pearson and Palmer 1999, 2000; Pagani et al. 2005). An increase in atmospheric CO_2 results in increased dissolved CO_2 in ocean water, which in turn causes a reduction in oceanic pH. A note of caution was presented by Lemarchand et al. (2000) who suggested that boron isotope variations in foraminifera depend at least in part on variations in the supply of riverine boron to the ocean during the geologic past. And indeed the boron isotope composition of rivers can be extremely variable (Rose et al. 2000; Lemarchand et al. 2002). Joachimski et al. (2005) presented evidence

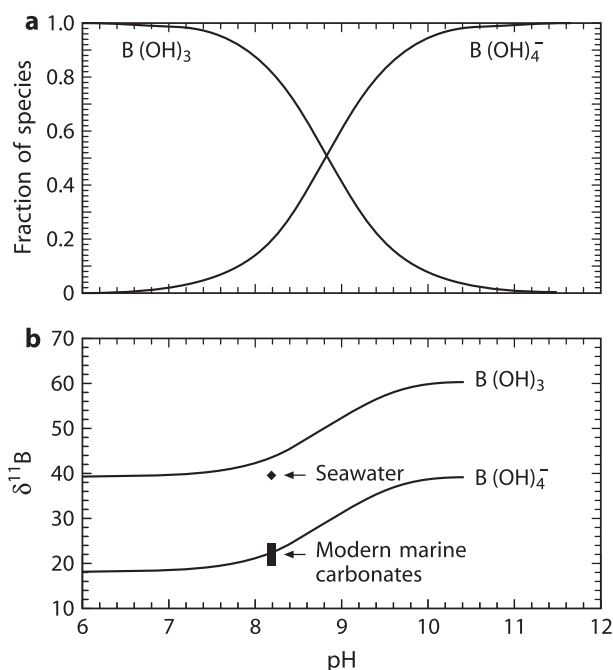


Fig. 2.8 (a) Distribution of aqueous boron species versus pH; (b) $\delta^{11}B$ of the two dominant species $B(OH)_3$ and $B(OH)_4^-$ versus pH (after Hemming and Hanson, 1992)

that Paleozoic oceans were lower in $\delta^{11}B$ by up to 10‰, which supports conclusions that boron isotope ratios cannot be used as a reliable paleo-pH indicator.

Fluid-rock interactions

Boron and – as already demonstrated – lithium are useful tracers for mass transfer estimates in subduction zones. Both elements are mobilized by fluids and melts and display considerable isotope fractionation during dehydration reactions. Concentrations of B and Li are low in mantle derived materials, whereas they are high in sediments, altered oceanic crust and continental crust. Any input of fluid and melt from the subducting slab into the overlying mantle has a strong impact on the isotope composition of the mantle wedge and on magmas generated there. Experimental studies of boron isotope fractionation between hydrous fluids, melts and minerals have shown that ^{11}B preferentially partitions into the fluid relative to minerals or melts (Palmer et al. 1987; Williams et al. 2001; Wunder et al. 2005; Liebscher et al. 2005), ranging from about 33‰ for fluid–clay (Palmer et al. 1987) to about 6‰ for fluid–muscovite at 700°C (Wunder et al. 2005) and to a few ‰ for fluid–melt above 1,000°C (Hervig et al. 2002). The main fractionation effect seems to be due to the change from trigonal boron in neutral pH hydrous fluid to tetrahedrally coordinated boron in most rock forming minerals.

Tourmaline

Tourmaline is the most abundant reservoir of boron in metamorphic and magmatic rocks. It is stable over a very large p - T range. Since volume diffusion of B isotopes is insignificant in tourmalines (Nakano and Nakamura 2001), isotopic heterogeneities of zoned tourmalines should be preserved up to at least 600°C. Swihart and Moore (1989), Palmer and Slack (1989), Slack et al. (1993), Smith and Yardley (1996) and Jiang and Palmer (1998) analyzed tourmaline from various geological settings and observed a large range in $\delta^{11}\text{B}$ -values which reflects the different origins of boron and its high mobility during fluid related processes. By using the SIMS method, Marschall et al. (2008) demonstrated that boron isotopes in zoned tourmalines indeed may reflect different stages of tourmaline growth.

Because tourmaline is usually the only boron-bearing mineral of significance, recrystallization of tourmaline will not produce any change in its ^{11}B -content, unless boron is lost or gained by the system. If boron is lost from the rock, the $\delta^{11}\text{B}$ -value of the recrystallized tourmaline will be lower than the original value because ^{11}B is preferentially partitioned into the fluid phase. Meyer et al. (2008) experimentally determined the boron partitioning between tourmaline and fluid. In the temperature range from 400 to 700°C ^{11}B preferentially fractionates into the fluid, but to a smaller degree than determined by Palmer et al. (1992).

2.4 Carbon

Carbon occurs in a wide variety of compounds on Earth, from reduced organic compounds in the biosphere to oxidized inorganic compounds like CO_2 and carbonates. The broad spectrum of carbon-bearing compounds involved in low- and high-temperature geological settings can be assessed on the basis of carbon isotope fractionations.

Carbon has two stable isotopes (Rosman and Taylor 1998)

$^{12}\text{C} = 98.93\%$ (reference mass for atomic weight scale)

$^{13}\text{C} = 1.07\%$

The naturally occurring variations in carbon isotope composition are greater than 120‰, neglecting extraterrestrial materials. Heavy carbonates with $\delta^{13}\text{C}$ -values $> +20\text{‰}$ and light methane of $< -100\text{‰}$ have been reported in the literature.

2.4.1 Preparation Techniques

The gases used in $^{13}\text{C}/^{12}\text{C}$ measurements are CO_2 and recently CO during pyrolysis applications. For CO_2 the following preparation methods exist:

1. Carbonates are reacted with 100% phosphoric acid at temperatures between 20 and 90°C (depending on the type of carbonate) to liberate CO_2 (see also “oxygen”).

2. Organic compounds are generally oxidized at high temperatures (850–1,000°C) in a stream of oxygen or by an oxidizing agent like CuO. In the last few years, a new methodology to measure ^{13}C -contents of individual compounds in complex organic mixtures has been developed. This so-called GC–C–MS technique employs a capillary column gas chromatograph, a combustion interface to produce CO_2 and a modified conventional gas mass–spectrometer and can measure individual carbon compounds in mixtures of sub-nanogram samples with a precision of better than $\pm 0.5\%$.

2.4.2 Standards

As the commonly used international reference standard PDB has been exhausted for several decades, there is a need for introducing new standards. Even though several different standards are in use today, the international standard the δ -values are referred to remains to be the PDB-standard (Table 2.2).

2.4.3 Fractionation Processes

The two main terrestrial carbon reservoirs, organic matter and sedimentary carbonates, have distinctly different isotopic characteristics because of the operation of two different reaction mechanisms:

1. Isotope equilibrium exchange reactions within the inorganic carbon system “atmospheric CO_2 – dissolved bicarbonate – solid carbonate” lead to an enrichment of ^{13}C in carbonates.
 2. Kinetic isotope effects during photosynthesis concentrate the light isotope ^{12}C in the synthesized organic material.
1. The inorganic carbonate system is comprised of multiple chemical species linked by a series of equilibria:

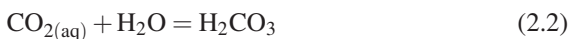
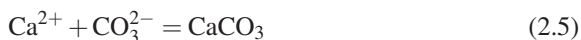


Table 2.2 $\delta^{13}\text{C}$ -values of NBS-reference samples relative to PDB

NBS-18	Carbonatite	–5.00
NBS-19	Marble	+1.95
NBS-20	limestone	–1.06
NBS-21	Graphite	–28.10

The carbonate (CO_3^{2-}) ion can combine with divalent cations to form solid minerals, calcite and aragonite being the most common



An isotope fractionation is associated with each of these equilibria, the ^{13}C -differences between the species depend only on temperature, although the relative abundances of the species are strongly dependent on pH. Several authors have reported isotope fractionation factors for the system dissolved inorganic carbon (DIC) – gaseous CO_2) (Vogel et al. 1970; Mook et al. 1974; Zhang et al. 1995). The major problem in the experimental determination of the fractionation factor is the separation of the dissolved carbon phases ($\text{CO}_{2\text{aq}}$, HCO_3^{3-} , CO_3^{3-}) because isotope equilibrium among these phases is reached within seconds. Figure 2.9 summarizes carbon isotope fractionations between various geologic materials and gaseous CO_2 (after Chacko et al. 2001).

The generally accepted carbon isotope equilibrium values between calcium carbonate and dissolved bicarbonate are derived from inorganic precipitate data of Rubinson and Clayton (1969), Emrich et al. (1970), and Turner (1982). What is often not adequately recognized is the fact that systematic C-isotope differences exist between calcite and aragonite. Rubinson and Clayton (1969) and Romanek et al. (1992) found calcite and aragonite to be 0.9 and 2.7‰ enriched in ^{13}C relative to bicarbonate at 25°C. Another complicating factor is that shell carbonate – precipitated by marine organisms – is frequently not in isotopic equilibrium with the ambient dissolved bicarbonate. Such so-called “vital” effects can be as large as a few permil (see discussion on p. 198).

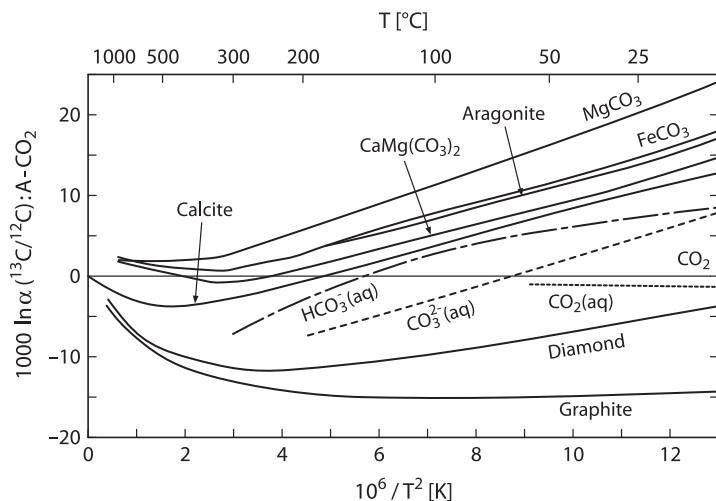


Fig. 2.9 Carbon isotope fractionations between various geologic materials and CO_2 (after Chacko et al. 2001)

Carbon isotope fractionations under equilibrium conditions are important not only at low-temperature, but also at high temperatures within the system carbonate, CO₂, graphite, and CH₄. Of these, the calcite-graphite fractionation has become a useful geothermometer (e.g., Valley and O'Neil 1981; Scheele and Hoefs 1992; Kitchen and Valley 1995) (see discussion on p. 227).

2. Early reviews by O'Leary (1981) and Farquhar et al. (1989) have provided the biochemical background of carbon isotope fractionations during photosynthesis, with more recent accounts by Hayes (2001) and Freeman (2001).

The main isotope-discriminating steps during biological carbon fixation are (1) the uptake and intracellular diffusion of CO₂ and (2) the biosynthesis of cellular components. Such a two-step model was first proposed by Park and Epstein (1960):



From this simplified scheme, it follows that the diffusional process is reversible, whereas the enzymatic carbon fixation is irreversible. The two-step model of carbon fixation clearly suggests that isotope fractionation is dependent on the partial pressure of CO₂, i.e. pCO₂ of the system. With an unlimited amount of CO₂ available to a plant, the enzymatic fractionation will determine the isotopic difference between the inorganic carbon source and the final bioproduct. Under these conditions, ¹³C fractionations may vary from -17 to -40‰ (O'Leary 1981). When the concentration of CO₂ is the limiting factor, the diffusion of CO₂ into the plant is the slow step in the reaction and carbon isotope fractionation of the plant decreases.

Atmospheric CO₂ first moves through the stomata, dissolves into leaf water and enters the outer layer of photosynthetic cells, the mesophyll cell. Mesophyll CO₂ is directly converted by the enzyme ribulose biphosphate carboxylase/oxygenase ("Rubisco") to a six carbon molecule that is then cleaved into two molecules of phosphoglycerate (PGA), each with three carbon atoms (plants using this photosynthetic pathway are therefore called C₃ plants). Most PGA is recycled to make ribulose biphosphate, but some is used to make carbohydrates. Free exchange between external and mesophyll CO₂ makes the carbon fixation process less efficient, which causes the observed large ¹³C-depletions of C₃ plants.

C₄ plants incorporate CO₂ by the carboxylation of phosphoenolpyruvate (PEP) via the enzyme PEP carboxylase to make the molecule oxaloacetate which has 4 carbon atoms (hence C₄). The carboxylation product is transported from the outer layer of mesophyll cells to the inner layer of bundle sheath cells, which are able to concentrate CO₂, so that most of the CO₂ is fixed with relatively little carbon fractionation.

In conclusion, the main controls on carbon fractionation in plants are the action of a particular enzyme and the "leakiness" of cells. Because mesophyll cells are permeable and bundle sheath cells are less permeable, C₃ vs C₄ plants have ¹³C-depletions of -18‰ versus -4‰ relative to atmospheric CO₂ (see Fig. 2.10).

Work summarized by Hayes (1993) and Hayes (2001) has demonstrated that the final carbon isotope composition of naturally synthesized organic matter depends on a complex set of parameters. (1) the ¹³C-content of the carbon source, (2) isotope

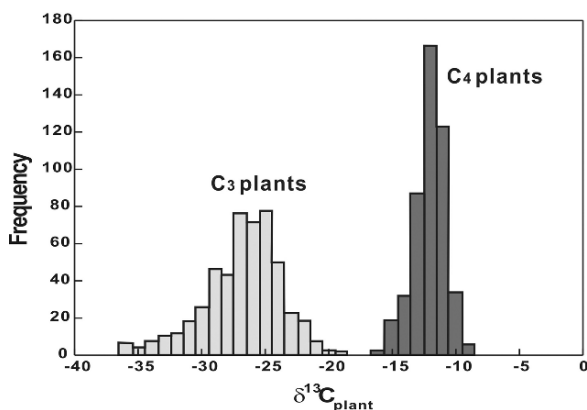


Fig. 2.10 Histogram of $\delta^{13}\text{C}$ -values of C_3 and C_4 plants (after Cerling and Harris, 1999)

effects associated with the assimilation of carbon, (3) isotope effects associated with metabolism and biosynthesis and (4) cellular carbon budgets.

Even more complex is C-isotope fractionation in aquatic plants. Factors that control the $\delta^{13}\text{C}$ of phytoplankton include temperature, availability of $\text{CO}_2(\text{aq})$, light intensity, nutrient availability, pH and physiological factors such as cell size and growth rate (Laws et al. 1995, 1997; Bidigare et al. 1997; Popp et al. 1998 and others). In particular the relationship between C-isotope composition of phytoplankton and concentration of oceanic dissolved CO_2 has been subject of considerable debate because of its potential as a palaeo- CO_2 barometer (see discussion).

Since the pioneering work of Park and Epstein (1960) and Abelson and Hoering (1961) it is well known that ^{13}C is not uniformly distributed among the total organic matter of plant material, but varies between carbohydrates, proteins and lipids. The latter class of compounds is considerably depleted in ^{13}C relative to the other products of biosynthesis. Although the causes of these ^{13}C -differences are not entirely clear, kinetic isotope effects seem to be more plausible (De Niro and Epstein 1977; Monson and Hayes 1982) than thermodynamic equilibrium effects (Galimov 1985a, 2006). The latter author argued that ^{13}C -concentrations at individual carbon positions within organic molecules are principally controlled by structural factors. Approximate calculations suggested that reduced C – H bonded positions are systematically depleted in ^{13}C , while oxidized C – O bonded positions are enriched in ^{13}C . Many of the observed relationships are qualitatively consistent with that concept. However, it is difficult to identify any general mechanism by which thermodynamic factors should be able to control chemical equilibrium within a complex organic structure. Experimental evidence presented by Monson and Hayes (1982) suggests that kinetic effects will be dominant in most biological systems.

2.4.4 Interactions between the Carbonate-Carbon Reservoir and Organic Carbon Reservoir

Variations in ^{13}C content of some important carbon compounds are schematically demonstrated in Fig. 2.11: The two most important carbon reservoirs on Earth, marine carbonates and the biogenic organic matter, are characterized by very different isotopic compositions: the carbonates being isotopically heavy with a mean $\delta^{13}\text{C}$ -value around 0‰ and organic matter being isotopically light with a mean $\delta^{13}\text{C}$ -value around -25‰. For these two sedimentary carbon reservoirs an isotope mass balance must exist such that:

$$\delta^{13}\text{C}_{\text{input}} = f_{\text{org}}\delta^{13}\text{C}_{\text{org}} + (1 - f_{\text{org}})\delta^{13}\text{C}_{\text{carb}} \quad (2.6)$$

If δ input, δ_{org} , δ_{carb} can be determined for a specific geologic time, f_{org} can be calculated, where f_{org} is the fraction of organic carbon entering the sediments. It should be noted that f_{org} is defined in terms of the global mass balance and is independent of biological productivity referring to the burial rather than the synthesis of organic material. That means that large f_{org} values might be a result of high productivity and average levels of preservation of organic material or of low levels of productivity and high levels of preservation.

The $\delta^{13}\text{C}$ -value for the input carbon cannot be measured precisely but can be estimated with a high degree of certainty. As will be shown later, mantle carbon has an isotopic composition around -5‰ and estimates of the global average isotope composition for crustal carbon also fall in that range. Assigning -5‰ to $\delta^{13}\text{C}$ -input, a modern value for f_{org} is calculated as 0.2 or expressed as the ratio of $\text{C}_{\text{org}}/\text{C}_{\text{carb}} = 20/80$. As will be shown later (Chapter) f_{org} has obviously changed during specific periods of the Earth's history (e.g. Hayes et al. 1999). With each molecule of organic carbon being buried, a mole of oxygen is released to the atmo-

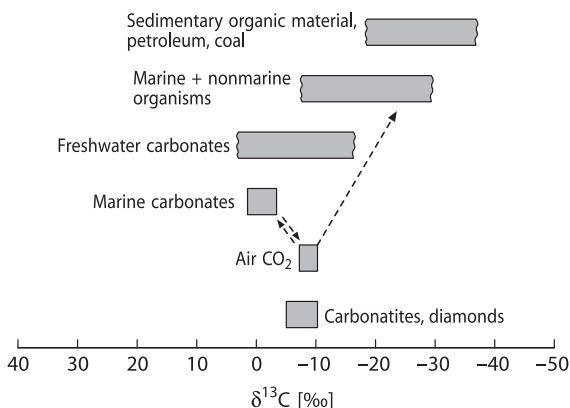


Fig. 2.11 $\delta^{13}\text{C}$ -values of some important carbon reservoirs

sphere. Hence, knowledge of f_{org} is of great value in reconstructing the crustal redox budget.

2.5 Nitrogen

More than 99% of the known nitrogen on or near the Earth's surface is present as atmospheric N_2 or as dissolved N_2 in the ocean. Only a minor amount is combined with other elements, mainly C, O, and H. Nevertheless, this small part plays a decisive role in the biological realm. Since nitrogen occurs in various oxidation states and in gaseous, dissolved, and solid forms (N_2 , NO_3^- , NO_2^- , NH_3 , NH_4^+), it is a highly suitable element for the search of natural variations in its isotopic composition. Schoenheimer and Rittenberg (1939) were the first to report nitrogen isotopic variations in biological materials. Today, the range of reported $\delta^{15}\text{N}$ -values covers 100‰, from about -50 to $+50$ ‰. However, most δ -values fall within the much narrower spread from -10 to $+20$ ‰, as described in more recent reviews of the exogenic nitrogen cycle by Heaton (1986), Owens (1987), Peterson and Fry (1987) and Kendall (1998).

Nitrogen consists of two stable isotopes, ^{14}N and ^{15}N . Atmospheric nitrogen, given by Rosman and Taylor (1998) has the following composition:

^{14}N : 99.63%

^{15}N : 0.37% .

N_2 is used for $^{15}\text{N}/^{14}\text{N}$ isotope ratio measurements, the standard is atmospheric N_2 . Various preparation procedures have been described for the different nitrogen compounds (Bremner and Keeney 1966; Owens 1987; ? ?; Kendall and Grim 1990; Scholten 1991 and others). In the early days of nitrogen isotope investigations the extraction and combustion techniques potentially involved chemical treatments that could have introduced isotopic fractionations. In recent years, simplified techniques for combustion have come into routine use, so that a precision of 0.1–0.2‰ for $\delta^{15}\text{N}$ determinations can be achieved. Organic nitrogen-compounds are combusted to CO_2 , H_2O and N_2 , the product gases are separated from each other cryogenically and the purified N_2 is trapped on molecular sieves for mass-spectrometric analysis.

To understand the processes leading to the nitrogen isotope distribution in the geological environment, a short discussion of the biological nitrogen cycle is required. Atmospheric nitrogen, the most abundant form of nitrogen, is the least reactive species of nitrogen. It can, however, be converted to “fixed” nitrogen by bacteria and algae, which, in turn, can be used by biota for degradation to simple nitrogen compounds such as ammonium and nitrate. Thus, microorganisms are responsible for all major conversions in the biological nitrogen cycle, which generally is divided into fixation, nitrification, and denitrification. Other bacteria return nitrogen to the atmosphere as N_2 .

The term *fixation* is used for processes that convert unreactive atmospheric N_2 into reactive nitrogen such as ammonium, usually involving bacteria. Fixation commonly produces organic materials with $\delta^{15}N$ -values slightly less than 0‰ ranging from -3 to $+1$ (Fogel and Cifuentes 1993) and occurs in the roots of plants by many bacteria. The large amount of energy needed to break the molecular nitrogen bond makes nitrogen fixation a very inefficient process with little associated N-isotope fractionation.

Nitrification is a multi-step oxidation process mediated by several different autotrophic organisms. Nitrate is not the only product of nitrification, different reactions produce various nitrogen oxides as intermediate species. Nitrification can be described as two partial oxidation reactions, each of which proceeds separately.

Oxidation by Nitrosomas ($NH_4 \rightarrow NO_2^-$) followed by oxidation by Nitrobacter ($NO_2^- \rightarrow NO_3^-$). Because the oxidation of nitrite to nitrate is generally rapid, most of the N-isotope fractionations is caused by the slow oxidation of ammonium by Nitrosomas. In N-limited systems fractionations are minimal.

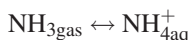
Denitrification (reduction of more oxidized forms to more reduced forms of nitrogen) is a multi-step process with various nitrogen oxides as intermediate compounds resulting from biologically mediated reduction of nitrate. Denitrification takes place in poorly aerated soil and in stratified anaerobic water bodies. Denitrification supposedly balances the natural fixation of nitrogen, if it did not occur, then atmospheric nitrogen would be exhausted in less than 100 million years. Denitrification causes the $\delta^{15}N$ -values of the residual nitrate to increase exponentially as nitrate concentrations decrease. Experimental investigations have demonstrated that fractionation factors may change from 10 to 30‰, with the largest values obtained under lowest reduction rates. Generally, the same factors that influence isotope fractionation during bacterial sulfate reduction are also operative during bacterial denitrification. Table 2.3, which gives a summary of observed N-isotope fractionations, clearly indicates the dependence of fractionations on nitrogen concentrations and

Table 2.3 Naturally observed isotope fractionation for nitrogen assimilation (after Fogel and Cifuentes Fogel and Cifuentes 1993)

N_2 fixation	-3 to $+1‰$
NH_4^+ assimilation	
Cultures	
Millimolar concentrations	0 to $-15‰$
Micromolar concentrations	-3 to $-27‰$
Field observations	
Micromolar concentrations	$-10‰$
NO_3^- assimilation	
Cultures	
Millimolar concentrations	0 to $-24‰$
Micromolar concentrations	$-10‰$
Field observations	
Micromolar concentrations	-4 to $-5‰$

demonstrates, that at low nitrogen concentrations fractionations are nearly zero because virtually all the nitrogen is used.

So far, only kinetic isotope effects have been considered, but isotopic fractionations associated with equilibrium exchange reactions have been demonstrated for the common inorganic nitrogen compounds (Letolle 1980). Of special importance in this respect is the ammonia volatilization reaction:



for which isotope fractionation factors of 1.025–1.035 have been determined (Kirshenbaum et al. 1947; Mariotti et al. 1981). Experimental data by Nitzsche and Stiehl (1984) indicate fractionation factors of 1.0143 at 250°C and of 1.0126 at 350°C very small ^{15}N -enrichment of about 0.1‰ occurs during the solution of atmospheric N_2 in ocean water (Benson and Parker 1961).

Nitrogen isotope studies are extremely important for evaluating the source and fate of nitrogen in the marine and terrestrial environment. $\delta^{15}\text{N}$ -values measured in the water column of the ocean and in sediments depend on the many nitrogen isotope fractionation reactions in the biological cycle. Nitrogen isotopes have been used as a paleoceanographic proxy, because they record changes of nutrient dynamics and ventilation that affects denitrification in the water column (e.g. Farrell et al. 1995). This approach is based on the fact that particulate organic nitrogen depends on (1) the isotopic composition of dissolved nitrate, which in oxygenated waters has a $\delta^{15}\text{N}$ -value of about –6‰ (in anoxic waters where denitrification occurs the $\delta^{15}\text{N}$ -value is significantly higher, up to 18.8‰ in the tropical North Pacific; Cline and Kaplan 1975) and on (2) isotope fractionation that occurs during nitrogen uptake by phytoplankton. In the photic zone phytoplankton preferentially incorporates ^{14}N , which results in a corresponding ^{15}N -enrichment in the residual nitrate. The N-isotope composition of settling organic detritus thus varies depending on the extent of nitrogen utilization: low ^{15}N contents indicate low relative utilisation, high ^{15}N contents indicate a high utilization.

Much of the initial organic nitrogen reaching the sediment/water interface is lost during early diagenesis. Nevertheless the nitrogen isotope composition of sediments is primarily determined by the source organic matter. Source studies have been undertaken to trace the contribution of terrestrial organic matter to ocean water and to sediments (i.e. Sweeney et al. 1978; Sweeney and Kaplan 1980). Such studies are based, however, on the assumption that the ^{15}N content remains unchanged in the water column. Investigations by Cifuentes et al. (1989), Altabet et al. (1991), and Montoya et al. (1991) have demonstrated that there may be rapid temporal (even on a time scale of days) and spatial changes in the nitrogen isotope composition of the water column due to biogeochemical processes. This complicates a clear distinction between terrestrial and marine organic matter, although marine organic matter generally has a higher $^{15}\text{N}/^{14}\text{N}$ ratio than terrestrial organic matter.

The organic matter in sediments has a mean $\delta^{15}\text{N}$ -value of around +7‰ (Sweeney et al. 1978). During diagenesis biological and thermal degradation of

the organic matter results in the formation of ammonium (NH_4) which can be incorporated for potassium in clay minerals. This nitrogen in the crystal lattice of clay minerals and micas is mainly derived from decomposing organic matter and thus has a very similar isotopic composition as the organic matter (Scholten 1991; Williams et al. 1995).

During metamorphism of sediments, there is a significant loss of ammonium during devolatilisation, which is associated with a nitrogen fractionation, leaving behind ^{15}N residues (Haendel et al. 1986; Bebout and Fogel 1992; Jia 2006). Thus high-grade metamorphic rocks and granites are relatively enriched in ^{15}N and typically have $\delta^{15}\text{N}$ -values between 8 and 10‰. Sadofsky and Bebout (2000) have examined the nitrogen isotope fractionation among coexisting micas, but could not find any characteristic difference between biotite and white mica.

In summary, nitrogen in sediments and crustal rocks exhibits positive $\delta^{15}\text{N}$ -values around 6‰. In contrast, mantle nitrogen extracted from MORB glasses (Marty and Humbert 1997; Marty and Zimmermann 1999) and from diamonds (Javoy et al. 1986; Cartigny et al. 1997) have average $\delta^{15}\text{N}$ -values of around -5‰. These similar values for subcontinental and MORB mantle suggests a homogeneous distribution of nitrogen isotopes in the mantle. $\delta^{15}\text{N}$ -values thus are an important tracer to distinguish mantle-derived from crustal derived nitrogen.

Many studies have shown that nitrogen isotopes can be used in environmental studies. Fertilizer, animal wastes or sewage are the main sources of nitrate pollution in the hydrosphere. Under favorable conditions, these N-bearing compounds can be isotopically distinguished from each other (Heaton 1986). Anthropogenic fertilizers have $\delta^{15}\text{N}$ -values in the range -4 to +4‰ reflecting their atmospheric source, whereas animal waste typically has $\delta^{15}\text{N}$ -values > 5‰. Soil-derived nitrate and fertilizer nitrate commonly have overlapping $\delta^{15}\text{N}$ -values. $\delta^{15}\text{N}$ can potentially also be used as trophic level indicator.

Figure 2.12 gives an overview about the nitrogen isotope variations in some important reservoirs.

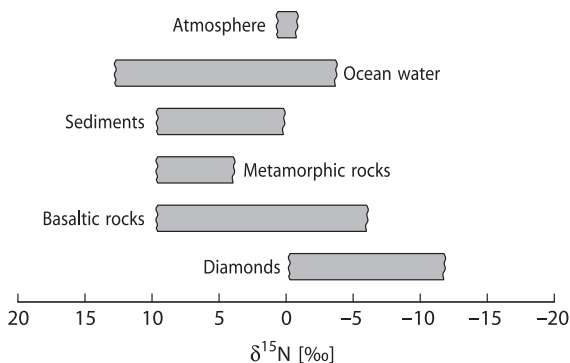


Fig. 2.12 $\delta^{15}\text{N}$ -values of geologically important reservoirs

2.6 Oxygen

Oxygen is the most abundant element on Earth. It occurs in gaseous, liquid and solid compounds, most of which are thermally stable over large temperature ranges. These facts make oxygen one of the most interesting elements in isotope geochemistry.

Oxygen has three stable isotopes with the following abundances (Rosman and Taylor 1998)

^{16}O : 99.757%

^{17}O : 0.038%

^{18}O : 0.205%

Because of the higher abundance and the greater mass difference, the $^{18}\text{O}/^{16}\text{O}$ ratio is normally determined, which may vary in natural samples by about 10% or in absolute numbers from about 1:475 to 1:525.

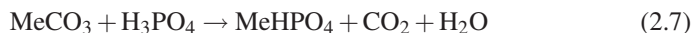
2.6.1 Preparation Techniques

CO_2 is the gas generally used for mass-spectrometric analysis. More recently CO and O_2 have also been used in high temperature conversion of organic material and in laser probe preparation techniques. A wide variety of methods have been described to liberate oxygen from the various oxygen-containing compounds.

Oxygen in silicates and oxides is usually liberated through fluorination with F_2 , BrF_5 or ClF_3 in nickel-tubes at 500 to 650°C (Taylor and Epstein 1962; Clayton and Mayeda 1963; Borthwick and Harmon 1982) or by heating with a laser (Sharp 1990). Decomposition by carbon reduction at 1,000 to 2,000°C may be suitable for quartz and iron oxides but not for all silicates (Clayton and Epstein 1958). The oxygen is converted to CO_2 over heated graphite or diamond. Care must be taken to ensure quantitative oxygen yields, which can be a problem in the case of highly refractive minerals like olivine and garnet. Low yields may result in anomalous $^{18}\text{O}/^{16}\text{O}$ ratios, high yields are often due to excess moisture in the vacuum extraction line.

Conventional fluorination is usually done on 10–20 mg of whole-rock powder or minerals separated from much larger samples; the inability to analyze small quantities means that natural heterogeneity cannot be detected by such bulk techniques. Recent advances in the development of laser microprobes, first described by Sharp (1990), have revolutionized mineral analyses. Laser techniques have both the resolution and precision to investigate isotopic zoning within single mineral grains and mineral inter- and overgrowths.

The standard procedure for the isotope analysis of carbonates is the reaction with 100% phosphoric acid at 25°C first described by McCrea (1950). The following reaction equation:



where Me is a divalent cation, shows that only two-thirds of the carbonate oxygen present in the product CO_2 is liberated, and thus a significant isotope effect is observed, which is on the order of 10‰, but varies up to a few ‰ depending on the cation, the reaction temperature and the preparation procedure. The so-called acid fractionation factor must be precisely known to obtain the oxygen isotope ratio of the carbonate. This can be done by measuring the $\delta^{18}\text{O}$ -value of the carbonate by fluorination with BrF_5 , first described by Sharma and Clayton (1965).

Experimental details of the phosphoric acid method vary significantly among different laboratories. The two most common varieties are the “sealed vessel” and the “acid bath” methods. In the latter method the CO_2 generated is continuously removed, while in the former it is not. Swart et al. (1991) demonstrated that the two methods exhibit a systematic ^{18}O difference between 0.2 and 0.4‰ over the temperature range 25 to 90°C. Of these the acid-bath method probably provides the more accurate results. A further modification of this technique is referred to as the “individual acid bath”, in which contaminations from the acid delivery system are minimized. Wachter and Hayes (1985) demonstrated that careful attention must be given to the phosphoric acid. In their experiments best results were obtained by using a 105% phosphoric acid and a reaction temperature of 75°C. This high reaction temperature should not be used when attempting to discriminate between mineralogically distinct carbonates by means of differential carbonate reaction rates.

Because some carbonates like magnesite or siderite react very sluggishly at 25°C, higher reaction temperatures are necessary to extract CO_2 from these minerals. Reaction temperatures have varied up to 90 or even 150°C (Rosenbaum and Sheppard 1986; Böttcher 1996), but there still exist considerable differences in the fractionation factors determined by various workers. For example fractionations between aragonite and calcite remain controversial and different workers have reported fractionations from negative to positive. Nevertheless there seems to be a general agreement that the fractionation factor for aragonite is about 0.6‰ higher than for calcite (Tarutani et al. 1969; Kim and O’Neil 1997), although Grossman and Ku (1986) have reported a value of up to 1.2‰. The dolomite-calcite fractionation may vary depending on specific composition (Land 1980). Table 2.4 reports acid fractionation factors for various carbonates.

Phosphates are first dissolved, then precipitated as silver phosphate (Crowson et al. 1991). Ag_3PO_4 is preferred because it is non-hygroscopic and can be precipitated rapidly without numerous chemical purification steps (O’Neil et al. 1994). This Ag_3PO_4 is then fluorinated (Crowson et al. 1991), reduced with C either in a furnace (O’Neil et al. 1994) or with a laser (Wenzel et al. 2000) or pyrolyzed (Vennemann et al. 2002). Because PO_4 does not exchange oxygen with water at room temperature (Kolodny et al. 1983), the isotopic composition of the Ag_3PO_4 is that of the PO_4 component of the natural phosphate. As summarized by Vennemann et al. (2002) conventional fluorination remains the most precise and accurate analytical technique for Ag_3PO_4 . Laser techniques on bulk materials have also been attempted (Cerling and Sharp 1996; Kohn et al. 1996; Wenzel et al. 2000), but because fossil phosphates invariably contain diagenetic contaminants, chemical processing and analysis of a specific component (CO_3 or PO_4) is ordinarily performed.

Table 2.4 Acid fractionation factors for various carbonates determined at 25°C (modified after Kim et al. 2007)

Mineral	α	Reference
Calcite	10.30	Kim et al. (2007)
Aragonite	10.63	Kim et al. (2007)
	11.14	Gilg (2007)
Dolomite	11.75	Rosenbaum and Sheppard (1986)
Magnesite	10.79 (50°C)	Das Sharma et al. (2002)
Siderite	11.63	Carothers et al. (1988)
Witherite	10.57	Kim and O'Neil (1997)

Sulfates are precipitated as BaSO_4 , and then reduced with carbon at 1,000°C to produce CO_2 and CO. The CO is either measured directly or converted to CO_2 by electrical discharge between platinum electrodes (Longinelli and Craig 1967). Total pyrolysis by continuous flow methods has made the analysis of sulfate oxygen more precise and less time-consuming than the off-line methods. Bao and Thiemens (2000) have used a CO_2 -laser fluorination system to liberate oxygen from barium sulfate.

The $^{18}\text{O}/^{16}\text{O}$ ratio of water is usually determined by equilibration of a small amount of CO_2 with a surplus of water at a constant temperature. For this technique the exact value of the fractionation for the $\text{CO}_2/\text{H}_2\text{O}$ equilibrium at a given temperature is of crucial importance. A number of authors have experimentally determined this fractionation at 25°C with variable results. A value of 1.0412 was proposed at the 1985 IAEA Consultants Group Meeting to be the best estimate.

It is also possible to quantitatively convert all water oxygen directly to CO_2 by reaction with guanidine hydrochloride (Dugan et al. 1985) which has the advantage that it is not necessary to assume a value for the $\text{H}_2\text{O} - \text{CO}_2$ isotope fractionation in order to obtain the $^{18}\text{O}/^{16}\text{O}$ ratio. On-line pyrolysis using TC-EA systems represents another approach (de Groot 2004).

2.6.2 Standards

Two different δ -scales are in use: $\delta^{18}\text{O}(\text{VSMOW})$ and $\delta^{18}\text{O}(\text{VPDB})$, because of two different categories of users, who have traditionally been engaged in O-isotope studies. The VPDB scale is used in low-temperature studies of carbonate. PDB is a Cretaceous belemnite from the Pee Dee Formation and was the laboratory working standard used at the university of Chicago in the early 1950's when the paleotemperature scale was developed. The original supply of this standard has long been exhausted, therefore secondary standards have been introduced (see Table 2.5), whose isotopic compositions have been calibrated relative to PDB. All other oxygen isotope analyses (waters, silicates, phosphates, sulfates, high-temperature carbonates) are given relative to SMOW.

Table 2.5 $\delta^{18}\text{O}$ -values of commonly used O-isotope standards

Standard	Material	PDB scale	VSMOW scale
NBS-19	Marble	-2.20	(28.64)
NBS-20	Limestone	-4.14	(26.64)
NBS-18	Carbonatite	-23.00	(7.20)
NBS-28	Quartz	(-20.67)	9.60
NBS-30	Biotite	(-25.30)	5.10
GISP	Water	(-53.99)	-24.75
SLAP	Water	(-83.82)	-55.50

The conversion equations of $\delta^{18}\text{O}(\text{PDB})$ versus $\delta^{18}\text{O}(\text{VSMOW})$ and vice versa (Coplen et al. 1983) are:

$$\delta^{18}\text{O}(\text{VSMOW}) = 1.03091\delta^{18}\text{O}(\text{PDB}) + 30.91$$

and

$$\delta^{18}\text{O}(\text{PDB}) = 0.97002\delta^{18}\text{O}(\text{VSMOW}) - 29.98$$

Table 2.5 gives the $\delta^{18}\text{O}$ -values of commonly used oxygen isotope standards on both scales (parenthesis denote calculated values).

2.6.3 Fractionation Processes

Out of the numerous possibilities to fractionate oxygen isotopes in nature, the following are of special significance.

Knowledge of the oxygen isotope fractionation between liquid water and water vapor is essential for the interpretation of the isotope composition of different water types. Fractionation factors experimentally determined in the temperature range from 0 to 350°C have been summarized by Horita and Wesolowski (1994). This is shown in Fig. 2.13.

Addition of salts to water also affects isotope fractionations. The presence of ionic salts in solution changes the local structure of water around dissolved ions. Taube (1954) first demonstrated that the $^{18}\text{O}/^{16}\text{O}$ ratio of CO_2 equilibrated with pure H_2O decreased upon the addition of MgCl_2 , AlCl_3 and HCl , remained more or less unchanged for NaCl , and increased upon the addition of CaCl_2 . The changes vary roughly linearly with the molality of the solute (see Fig. 2.14).

To explain this different fractionation behavior, Taube (1954) postulated different isotope effects between the isotopic properties of water in the hydration sphere of the cation and the remaining bulk water. The hydration sphere is highly ordered, whereas the outer layer is poorly ordered. The relative sizes of the two layers are dependent upon the magnitude of the electric field around the dissolved ions. The strength of the interaction between the dissolved ion and water molecules is also dependent upon the atomic mass of the atom to which the ion is bonded.

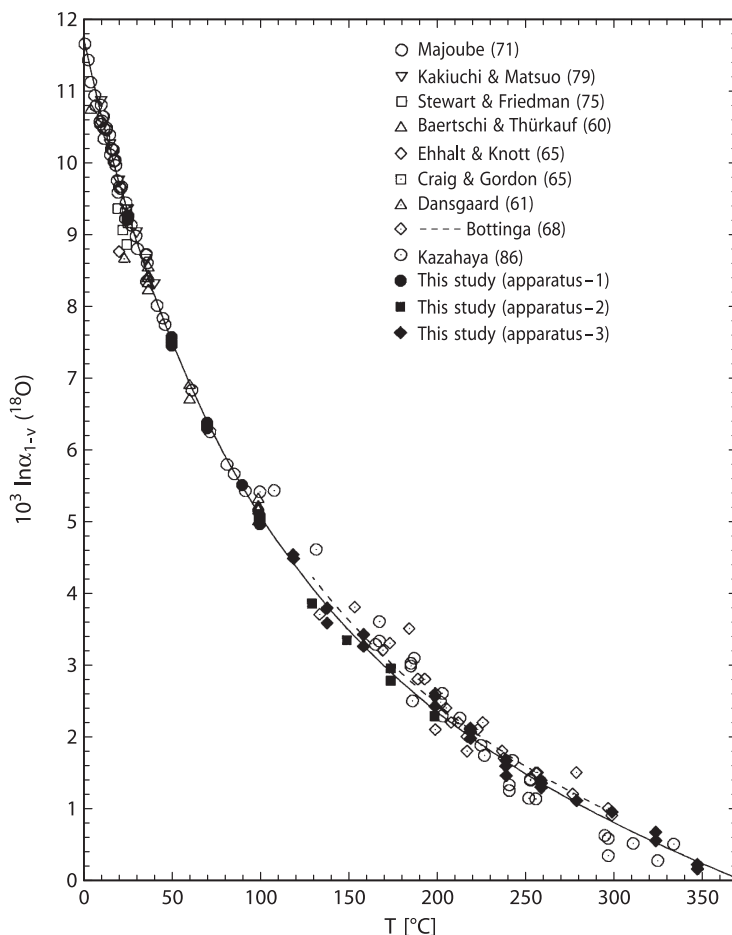


Fig. 2.13 Oxygen isotope fractionation factors between liquid water and water vapour in the temperature range 0 – 350°C (after Horita and Wesolowski 1994)

O’Neil and Truesdell (1991) have introduced the concept of “structure-making” and “structure-breaking” solutes: structure makers yield more positive isotope fractionations relative to pure water whereas structure breakers produce negative isotope fractionations. Any solute that results in a positive isotope fractionation is one that causes the solution to be more structured as is the case for ice structure, when compared to solutes that lead to less structured forms, in which cation – H₂O bonds are weaker than H₂O – H₂O bonds.

As already treated in the “hydrogen” section, isotope fractionations, the hydration of ions may play a significant role in hydrothermal solutions and volcanic vapors (Driesner and Seward 2000). Such isotope salt effects may change the oxygen isotope fractionation between water and other phases by several permil.

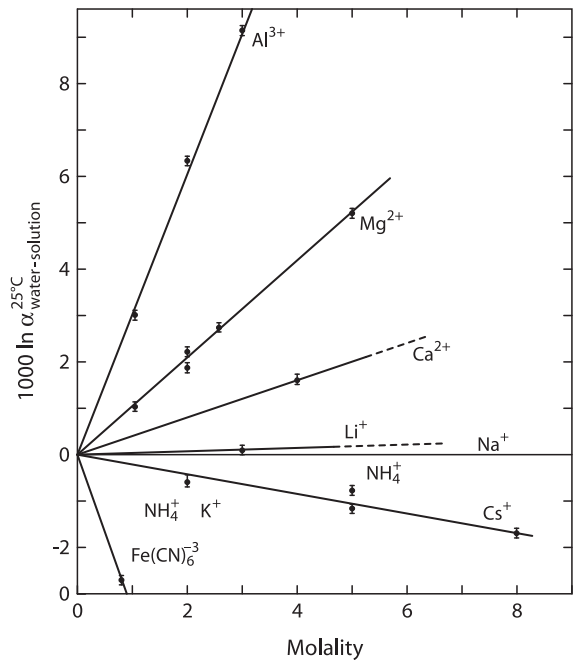


Fig. 2.14 Oxygen isotope fractionations between pure water and solutions of various ions (after O’Neil and Truesdell 1991)

Table 2.6 Experimentally determined oxygen isotope fractionation factors relative to water for the aqueous system CO₂ – H₂O between 5 and 40°C according to $10^3 \ln \alpha = A(10^6/T^{-2}) + B$ (Beck et al. 2005)

	A	B
HCO ₃ ⁻	2.59	1.89
CO ₃ ²⁻	2.39	-2.70
CO _{2(aq)}	2.52	12.12

Of equal importance is the oxygen isotope fractionation in the CO₂ – H₂O system. Early work concentrated on the oxygen isotope partitioning between gaseous CO₂ and water (Brennikmeijer et al. 1983). More recent work by Usdowski and Hoefs (1993), Beck et al. (2005) and Zeebe (2007) have determined the oxygen isotope composition of the individual carbonate species that are isotopically different at room temperature. Table 2.6 summarizes the equations for the temperature dependence between 5 and 40°C (Beck et al. 2005).

The fractionation (1,000 ln α) between dissolved CO₂ and water at 25°C is 41.6, dropping to 24.7 at high pH when CO₃²⁻ is the dominant species (see Fig. 2.15).

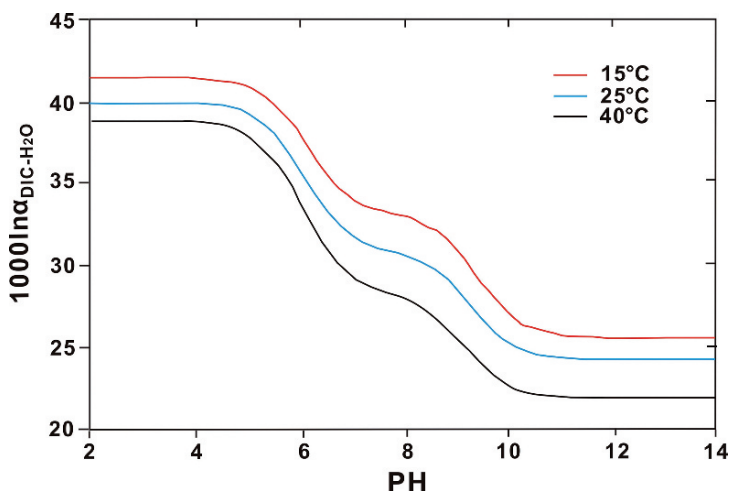


Fig. 2.15 Oxygen isotope fractionations between dissolved inorganic carbon (DIC) and water as a function of pH and temperatures (after Beck et al. 2005)

Table 2.7 Sequence of minerals in the order (bottom to top) of their increasing tendency to concentrate ^{18}O

Quartz
Dolomite
K-feldspar, albite
Calcite
Na-rich plagioclase
Ca-rich plagioclase
Muscovite, paragonite, kyanite, glaucophane
Orthopyroxene, biotite
Clinopyroxene, hornblende, garnet, zircon
Olivine
Ilmenite
Magnetite, hematite

The pH dependence of the oxygen isotope composition in the carbonate-water system has important implications in the derivation of oxygen isotope temperatures.

The oxygen isotope composition of a rock depends on the ^{18}O contents of the constituent minerals and the mineral proportions. Garlick (1966) and Taylor (1968) arranged coexisting minerals according to their relative tendencies to concentrate ^{18}O . The list given in Table 2.7 has been augmented by data from Kohn and Valley (1998a, b, c).

This order of decreasing ^{18}O -contents has been explained in terms of the bond-type and strength in the crystal structure. Semi-empirical bond-type calculations have been developed by Garlick (1966) and Savin and Lee (1988) by assuming that oxygen in a chemical bond has similar isotopic behavior regardless of the mineral in which the bond is located. This approach is useful for estimating fractionation

factors. The accuracy of this approach is limited due to the assumption that the isotope fractionation depends only upon the atoms to which oxygen is bonded and not upon the structure of the mineral, which is not strictly true. By using an electrostatic approximation to bond strength and taking into account cation mass Schütze (1980) developed an increment method for calculations of oxygen isotope fractionations in silicates, which has been modified and refined by Zheng (1991, 1993a, b). Kohn and Valley (1998a, b) determined empirically the effects of cation substitutions in complex minerals such as amphiboles and garnets spanning a large range in chemical compositions. Although isotope effects of cation exchange are generally less than 1‰ at $T > 500^\circ\text{C}$, they increase considerably at lower temperatures. Thus use of amphiboles and garnets for thermometry requires exact knowledge of chemical compositions.

On the basis of these systematic tendencies of ^{18}O enrichment found in nature, significant temperature information can be obtained up to temperatures of $1,000^\circ\text{C}$, and even higher, if calibration curves can be worked out for the various mineral pairs. The published literature contains many calibrations of oxygen isotope geothermometers, most are determined by laboratory experiments, although some are based on theoretical calculations.

Although much effort has been directed toward the experimental determination of oxygen isotope fractionation factors in mineral-water systems, the use of water as an oxygen isotope exchange medium has several disadvantages. Some minerals become unstable in contact with water at elevated temperatures and pressures, leading to melting, breakdown and hydration reactions. Incongruent solubility and ill-defined quench products may introduce additional uncertainties. Most of the disadvantages of water can be circumvented by using calcite as an exchange medium (Clayton et al. 1989; Chiba et al. 1989). Mineral-mineral fractionations – determined by these authors (Table 2.8) – give internally consistent geothermometric information that generally is in accord with independent estimates, such as the theoretical calibrations of Kieffer (1982).

A more recent summary has been given by Chacko et al. (2001) (see Fig. 2.16).

Many isotopic fractionations between low-temperature minerals and water have been estimated by assuming that their temperature of formation and the isotopic composition of the water in which they formed (for example, ocean water) are well known. This is sometimes the only approach available in cases in which the rates of

Table 2.8 Coefficients A for silicate – pair fractionations ($1,000 \ln \alpha_{X-Y} = A/T^2 \cdot 10^6$ (after Chiba et al. 1989)

	Cc	Ab	An	Di	Fo	Mt
Qtz	0.38	0.94	1.99	2.75	3.67	6.29
Cc		0.56	1.61	2.37	3.29	5.91
Ab			1.05	1.81	2.73	5.35
An				0.76	1.68	4.30
Di					0.92	3.54
Fo						2.62

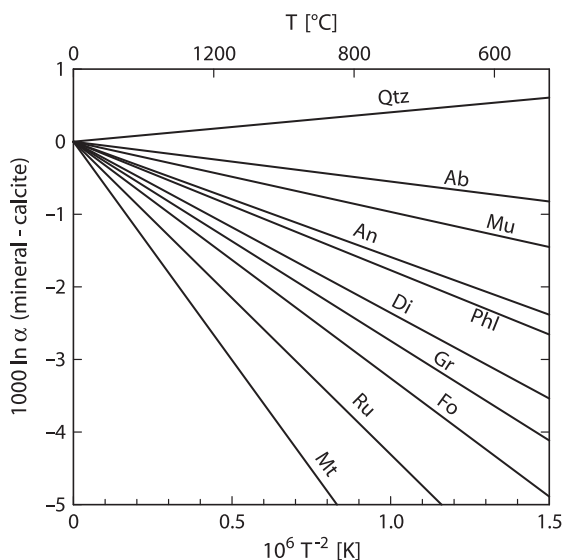


Fig. 2.16 Oxygen isotope fractionations between various minerals and calcite (after Chacko et al. 2001)

isotope exchange reactions are slow and in which minerals cannot be synthesized in the laboratory at appropriate temperatures.

2.6.4 Fluid-Rock Interactions

Oxygen isotope ratio analysis provides a powerful tool for the study of water/rock interaction. The geochemical effect of such an interaction between water and rock or mineral is a shift of the oxygen isotope ratios of the rock and/or the water away from their initial values, given that their compositions are not in equilibrium.

Detailed studies of the kinetics and mechanisms of oxygen isotope exchange between minerals and fluids show that there are three possible exchange mechanisms (Matthews et al. 1983b, c; Gilotti 1985).

1. *Solution-precipitation.* During a solution-precipitation process, larger grains grow at the expense of smaller grains. Smaller grains dissolve and recrystallize on the surface of larger grains which decreases the overall surface area and lowers the total free energy of the system. Isotopic exchange with the fluid occurs while material is in solution.
2. *Chemical reaction.* The chemical activity of one component of both fluid and solid is so different in the two phases that a chemical reaction occurs. The breakdown of a finite portion of the original crystal and the formation of new crystals is implied. The new crystals would form at or near isotopic equilibrium with the fluid.

3. *Diffusion*. During a diffusion process isotopic exchange takes place at the interface between the crystal and the fluid with little or no change in morphology of the reactant grains. The driving force is the random thermal motion of the atoms within a concentration or activity gradient.

In the presence of a fluid phase, coupled dissolution – reprecipitation is known to be a much more effective process than diffusion. This has been first demonstrated experimentally by O’Neil and Taylor (1967) and later re-emphasized by Cole (2000) and Fiebig and Hoefs (2002).

The first attempts to quantify isotope exchange processes between water and rocks were made by Taylor (1974). By using a simple closed-system material balance equation these authors were able to calculate cumulative fluid/rock ratios.

$$W/R = \frac{\delta_{\text{rock}_f} - \delta_{\text{rock}_i}}{\delta_{\text{H}_2\text{O}} - (\delta_{\text{rock}_f} - \Delta)}, \quad (2.8)$$

where $\Delta = \delta_{\text{rock}_f} - \delta_{\text{H}_2\text{O}_f}$.

Their equation requires adequate knowledge of both the initial (i) and final (f) isotopic states of the system and describes the interaction of one finite volume of rock with a fluid. The utility of such “zero-dimensional” equations has been questioned by Baumgartner and Rumble (1988), Blattner and Lassey (1989), Nabelek (1991), Bowman et al. (1994) and others. Only under special conditions do one-box models yield information on the amount of fluid that actually flowed through the rocks. If the rock and the infiltrating fluid were not far out of isotopic equilibrium, then the calculated fluid/rock ratios rapidly approach infinity. Therefore, the equations are sensitive only to small fluid/rock ratios. Nevertheless, the equations can constrain fluid sources. More sophisticated one-dimensional models like the chromatographic or continuum mechanics models (i.e. Baumgartner and Rumble 1988) are physically more plausible and can describe how the isotopic composition of the rock and of the fluid change with time and space. The mathematical models are complex and are based on partial differential equations that must be solved numerically. Examples of fluid–rock interactions in contact metamorphic environments have been presented by Nabelek and Labotka 1993, Bowman et al. 1994 and application to contrasting lithologies by Bickle and Baker (1990) and Cartwright and Valley (1991).

Criss et al. (1987) and Gregory et al. (1989) developed a theoretical framework that describes the kinetics of oxygen isotope exchange between minerals and co-existing fluids. Figure 2.17 shows characteristic patterns in δ - δ plots for some hydrothermally altered granitic and gabbroic rocks. The $^{18}\text{O}/^{16}\text{O}$ arrays displayed on Fig. 2.17 cut across the 45° equilibrium lines at a steep angle as a result of the much faster oxygen isotope exchange of feldspar compared to that of quartz and pyroxene. If a low- ^{18}O fluid such as meteoric or ocean water is involved in the exchange process, the slopes of the disequilibrium arrays can be regarded as “isochrons” where, with continued exchange through time the slopes become less steep and approach the 45° equilibrium line. These “times” represent the duration of a particular hydrothermal event.

Figure 2.18 summarizes the naturally observed oxygen isotope variations in important geological reservoirs.

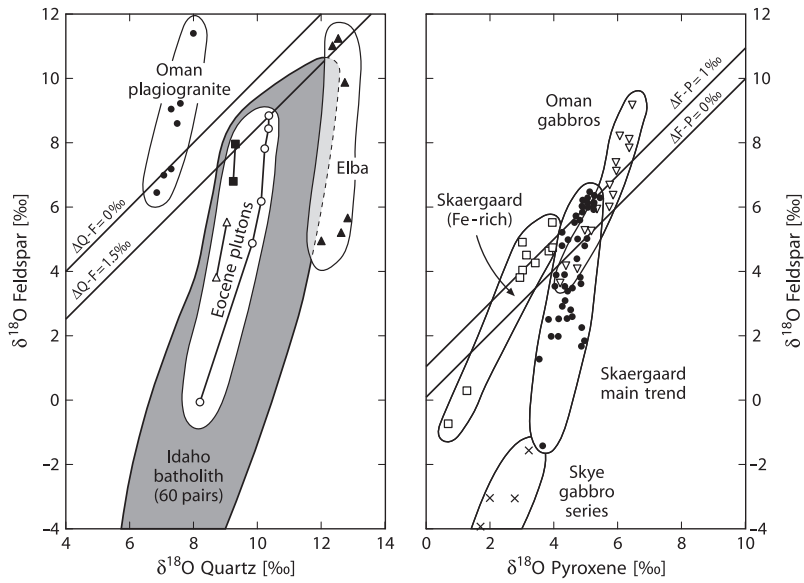


Fig. 2.17 $\delta^{18}\text{O}$ (feldspar) vs $\delta^{18}\text{O}$ (quartz) and vs $\delta^{18}\text{O}$ (pyroxene) plots of disequilibrium mineral pair arrays in granitic and gabbroic rocks. The arrays indicate open-system conditions from circulation of hydrothermal fluids (after Gregory et al. 1989)

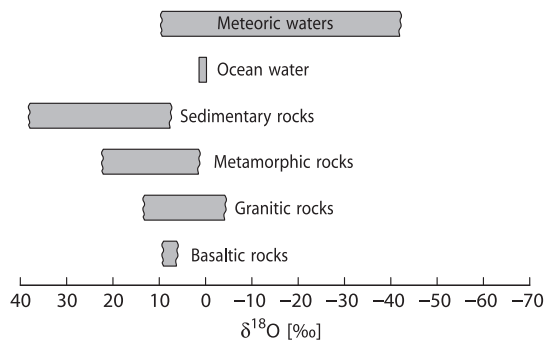


Fig. 2.18 $\delta^{18}\text{O}$ values of important geological reservoirs

2.7 Magnesium

Magnesium is composed of three isotopes (Rosman and Taylor 1998)

- ^{24}Mg 78.99%
- ^{25}Mg 10.00%
- ^{26}Mg 11.01%

Early investigations on Mg isotope variations have been limited by an uncertainty of 1 to 2‰. Catanzaro and Murphy (1966) for instance concluded that terrestrial Mg isotope variations are restricted to a few ‰. The introduction of multicollector-inductively coupled-plasma mass spectrometry (MC-ICP-MS) increased the precision by one order of magnitude and has initiated a new search of natural isotope variations (Galy et al. 2001, 2002). These authors obtained an overall 4‰ variation in $\delta^{26}\text{Mg}$.

The oxidation state of magnesium always is two, thus it might be expected that the range in isotope composition is small. Mg is soluble and mobile during weathering, which, on the other hand, might initiate small fractionations during carbonate precipitation and clay formation. And indeed by investigating Mg isotope fractionation between speleothems and associated drip waters Galy et al. (2002) observed a characteristic difference in both phases, which might indicate equilibrium conditions. They further observed a 2–3‰ enrichment in dolomites relative to limestones, suggesting a mineralogical control on the isotope composition of carbonates.

Because of its relatively long mean residence time, ocean water has a constant isotope composition. Corals are about 1‰ and foraminifera are about 4.5‰ lighter than ocean water. Thus significant Mg isotope fractionations occur during biomineralization of carbonate secreting organisms which is larger than for Ca isotopes (see Section 2.11).

Tipper et al. (2006) have measured the Mg isotope composition of rivers. They observed a total variation in ^{26}Mg of 2.5‰. The lithology in the drainage area seems to be of limited significance, a major part of the variability has to be attributed to fractionations in the weathering environment.

One of the advantages of the MC-ICPMS technique compared to the SIMS technique is the ability to measure $^{25}\text{Mg}/^{24}\text{Mg}$ and $^{26}\text{Mg}/^{24}\text{Mg}$ ratios independently many times smaller than the magnitude of the natural variations. By doing this Young and Galy (2004) demonstrated that the relationship between $^{25}\text{Mg}/^{24}\text{Mg}$ and $^{26}\text{Mg}/^{24}\text{Mg}$ are diagnostic of kinetic vs equilibrium fractionations: for equilibrium processes the slope on a three-isotope diagram should be close to 0.521, for kinetic processes the slope should be 0.511. Evidence for equilibrium fractionation has been found for low-Mg calcite speleothems (Galy et al. 2002). Recently, however, Buhl et al. (2007) argued that a pure equilibrium mass fractionation cannot explain the Mg isotope data from speleothems. On the other hand biologically mediated precipitates such as foraminifera (Chang et al. 2004) and dolomites of bacterial origin (Carder et al. 2005) have a clear kinetic signature.

Galy et al. (2001) suggested that the mantle should have a homogeneous Mg isotope composition. Pearson et al. (2006), however, demonstrated that olivines from mantle xenoliths have a heterogeneous compositions with a $\delta^{26}\text{Mg}$ range of about 4‰. These authors suggested that the differences are due to diffusion-related metasomatic processes.

2.8 Silicon

Silicon has three stable isotopes with the following abundances (Rosman and Taylor 1998):

^{28}Si 92.23%

^{29}Si 4.68%

^{30}Si 3.09%

Because of its high abundance on Earth, silicon is in principle a very interesting element to study for isotope variations. However, because there is no redox reaction for silicon (silicon is always bound to oxygen), only small isotope fractionations are to be expected in nature. Silicic acid, on the other hand, is an important nutrient in the ocean that is required for the growth of mainly diatoms and radiolaria. The silicon incorporation into siliceous organisms is associated with a Si isotope fractionation, because ^{28}Si is preferentially removed as the organisms form biogenic silica. Early investigations by Douthitt (1982) and more recent ones by Ding et al. (1996) observed a total range of $\delta^{30}\text{Si}$ values in the order of 6‰. This range has extended to about 12‰ with the lowest $\delta^{30}\text{Si}$ value of -5.7‰ in siliceous cements (Basile-Doelsch et al. 2005) and the highest of $+6.1\text{‰}$ for rice grains (Ding et al. 2005).

Silicon isotope ratios have been generally measured by fluorination (Douthitt 1982; Ding et al. 1996). However, the method is time consuming and potentially hazardous, therefore, more recently MC-ICP-MS techniques have been introduced (Cardinal et al. 2003; Engstrom et al. 2006). Determinations with SIMS have been carried out by Robert and Chaussidon (2006). Very recently, Chmeleff et al. (2008) have shown that a UV-femtosecond laser ablation system coupled with MC-ICP-MS gives $\delta^{29}\text{Si}$ and $\delta^{30}\text{Si}$ -values with very high precision.

Igneous rocks have a rather uniform isotope composition with a rather constant $\delta^{30}\text{Si}$ -value of -0.3‰ . In igneous rocks and minerals $\delta^{30}\text{Si}$ values exhibit small, but systematic variations with ^{30}Si enrichment increasing with the silicon contents of igneous rocks and minerals. The order of ^{30}Si enrichment is quartz, feldspar, muscovite and biotite, which is consistent with the order of ^{18}O enrichment. Thus felsic igneous rocks are slightly heavier than mafic igneous rocks.

Relative to igneous rocks rivers are isotopically enriched in ^{30}Si (De la Rocha et al. 2000a; Ding et al. 2004; Ziegler et al. 2005a, b; Basile-Doelsch et al. 2005; Reynolds et al. 2006; Georg et al. 2006). The enrichment in ^{30}Si is obviously produced during weathering which preferentially releases ^{28}Si into solution, followed by even stronger preferential incorporation of ^{28}Si during secondary mineral formation. Thus soil-clay mineral formation is responsible for high $\delta^{30}\text{Si}$ values of continental surface waters and ocean water. For the Yangtze river as an example, Ding et al. (2004) measured a $\delta^{30}\text{Si}$ range from 0.7 to 3.4‰ , whereas the suspended matter has a more constant composition from 0 to -0.7‰ .

In ocean water distinct ^{30}Si gradients with depth exist (Georg et al. 2006): surface waters are relatively rich in ^{30}Si whereas deep waters are more depleted in ^{30}Si , which is due to a silicon isotope fractionation during the uptake by organisms

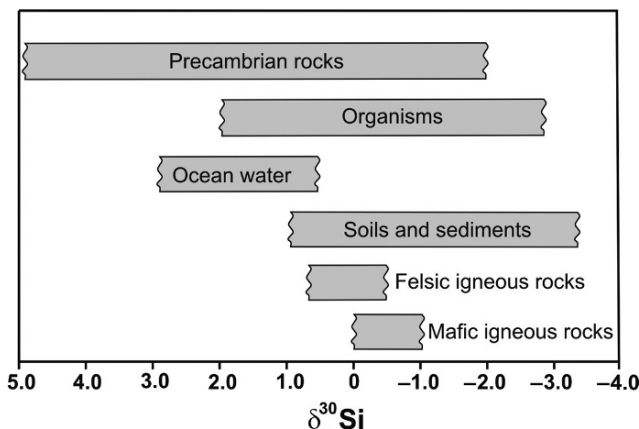


Fig. 2.19 $\delta^{30}\text{Si}$ ranges of various geologic reservoirs

in oceanic surface waters. De la Rocha et al. (1997, 1998) observed a 1‰ fractionation between dissolved and biogenic silica during opal formation by marine diatoms that does not vary with temperature nor among three species of diatoms. An increase in opal formation by diatoms results in more positive $\delta^{30}\text{Si}$ -values, whereas a decrease results in more negative δ -values. In this manner variations in ^{30}Si contents of diatoms may provide information on changes of oceanic silicon cycling (De la Rocha et al. 1998). Marine sponges fractionate silicon isotopes to a degree that is three times larger than observed by marine diatoms (De La Rocha 2003). Figure 2.19 summarizes natural silicon isotope variations.

A wide range of $\delta^{30}\text{Si}$ values from -0.8 to $+5.0$ ‰ have been reported for Precambrian cherts (Robert and Chaussidon 2006), much larger than for Phanerozoic cherts. These authors observed a positive correlation of $\delta^{18}\text{O}$ with $\delta^{30}\text{Si}$ values, which they interpreted as reflecting temperature changes in the ocean from about 70°C 3.5 Ga to about 20°C 0.8 Ga years ago.

2.9 Sulfur

Sulfur has four stable isotopes with the following abundances (Rosman and Taylor 1998)

^{32}S : 94.93%

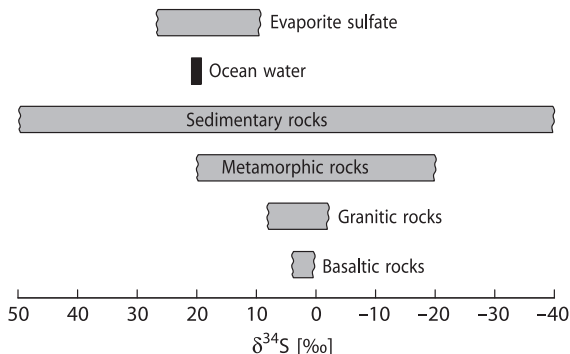
^{33}S : 0.76%

^{34}S : 4.29%

^{36}S : 0.02%

Sulfur is present in nearly all natural environments. It may be a major component in ore deposits, where sulfur is the dominant nonmetal, and as sulfates in evaporites. It occurs as a minor component in igneous and metamorphic rocks, throughout

Fig. 2.20 $\delta^{34}\text{S}$ -values of some geologically important sulfur reservoirs



the biosphere in organic substances, in marine waters and sediments as both sulfide and sulfate. These occurrences cover the whole temperature range of geological interest. Thus, it is quite clear that sulfur is of special interest in stable isotope geochemistry.

Thode et al. (1949) and Trofimov (1949) were the first to observe wide variations in the abundances of sulfur isotopes. Variations on the order of 180‰ have been documented with the “heaviest” sulfates having $\delta^{34}\text{S}$ -values of greater than +120‰ (Hoefs, unpublished results), and the “lightest” sulfides having $\delta^{34}\text{S}$ -values of around -65‰. Some of the naturally occurring S-isotope variations are summarized in Fig. 2.20. Reviews of the isotope geochemistry of sulfur have been published by Nielsen (1979), Ohmoto and Rye (1979), Ohmoto (1986), Ohmoto and Goldhaber (1997), Seal et al. (2000), Canfield (2001a) and Seal (2006).

For many years the reference standard commonly referred to is sulfur from troilite of the Canyon Diablo iron meteorite (CDT). As Beaudoin et al. (1994) have pointed out, CDT is not homogeneous and may display variations in ^{34}S up to 0.4‰. Therefore a new reference scale, Vienna-CDT or V-CDT has been introduced by an advisory committee of IAEA in 1993, recommending an artificially prepared Ag_2S (IAEA-S-1) with a $\delta^{34}\text{S}_{\text{VCDT}}$ of -0.3‰ as the new international standard reference material.

2.9.1 Preparation Techniques

Chemical preparation of the various sulfur compounds for isotopic analysis have been discussed by Rafter (1957), Robinson and Kusakabe (1975) among others. The gas generally used for mass-spectrometric measurement is SO_2 , although Puchelt et al. (1971) and Rees (1978) describe a method using SF_6 which has some distinct advantages: it has no mass spectrometer memory effect and because fluorine is monoisotopic, no corrections of the raw data of measured isotope ratios are necessary. Comparison of $\delta^{34}\text{S}$ -values obtained using the conventional SO_2 and the laser SF_6 technique has raised serious questions about the reliability of the SO_2

correction for oxygen isobaric interferences (Beaudoin and Taylor 1994). Therefore the SF₆ technique has been revitalized (Hu et al. 2003), demonstrating that SF₆ is an ideal gas for measuring $^{33}\text{S}/^{32}\text{S}$, $^{34}\text{S}/^{32}\text{S}$ and $^{36}\text{S}/^{32}\text{S}$ ratios.

For SO₂, pure sulfides have to be reacted with an oxidizing agent, like CuO, Cu₂O, V₂O₅ or O₂. It is important to minimize the production of sulfur trioxide since there is an isotope fractionation between SO₂ and SO₃. Special chemical treatment is necessary if pyrite is to be analyzed separately from other sulfides.

For the extraction of sulfates and total sulfur a suitable acid and reducing agent, such as tin(II)–phosphoric acid (the “Kiba” solution of Sasaki et al. 1979) is needed. The direct thermal reduction of sulfate to SO₂ has been described by Holt and Engelkemeier (1970) and Coleman and Moore (1978). Ueda and Sakai (1984) described a method in which sulfate and sulfide disseminated in rocks are converted to SO₂ and H₂S simultaneously, but analyzed separately. With the introduction of on-line combustion methods (Giesemann et al. 1994), multistep off-line preparations can be reduced to one single preparation step, namely the combustion in an elemental analyzer. Sample preparations have become less dependent on possibly fractionating wet-chemical extraction steps and less time-consuming.

Microanalytical techniques such as laser microprobe (Kelley and Fallick 1990; Crowe et al. 1990; Hu et al. 2003; Ono et al. 2006) and ion microprobe (Chaussidon et al. 1987, 1989; Eldridge et al. 1988, 1993) have become promising tools for determining sulfur isotope ratios. These techniques have several advantages over conventional techniques such as high spatial resolution and the capability for “in-situ” spot analysis. Sulfur isotopes are fractionated during ion or laser bombardment, but fractionation effects are mineral specific and reproducible.

2.9.2 Fractionation Mechanisms

Two types of fractionation mechanisms are responsible for the naturally occurring sulfur isotope variations:

1. Kinetic isotope effects during microbial processes. Micro-organisms have long been known to fractionate isotopes during their sulfur metabolism, particularly during dissimilatory sulfate reduction, which produces the largest fractionations in the sulfur cycle
2. Various chemical exchange reactions between both sulfate and sulfides and the different sulfides themselves

2.9.2.1 Dissimilatory Sulfate Reduction

Dissimilatory sulfate reduction is conducted by a large group of organisms (over 100 species are known so far, Canfield 2001a), that gain energy for their growth by reducing sulfate while oxidizing organic carbon (or H₂). Sulfate reducers are widely

distributed in anoxic environments. They can tolerate temperatures from -1.5 to over 100°C and salinities from fresh water to brines.

Since the early work with living cultures (Harrison and Thode 1957a, b; Kaplan and Rittenberg 1964) it is well known that sulfate reducing bacteria produce ^{32}S -depleted sulfide. Despite decades of intense research the factors that determine the magnitude of sulfur isotope fractionation during bacterial sulfate reduction are still under debate. The magnitude of isotope fractionation depends on the rate of sulfate reduction with the highest fractionation at low rates and the lowest fractionation at high rates. Kaplan and Rittenberg (1964) and Habicht and Canfield (1997) suggested that fractionations depend on the specific rate ($\text{cell}^{-1} \text{ time}^{-1}$) and not so much on absolute rates ($\text{volume}^{-1} \text{ time}^{-1}$). What is clear, however, is that the rates of sulfate reduction are controlled by the availability of dissolved organic compounds. One parameter which remains unclear is sulfate concentration. While for instance Boudreau and Westrich (1984) argued that the concentration of sulfate becomes important at rather low concentrations (less than 15% of the seawater value), Canfield (2001b) observed no influence of isotope fractionations on sulfate concentrations for natural populations. Another parameter, that has been thought to be important is temperature insofar as it regulates in natural populations the sulfate-reducing community (Brüchert et al. 2001). Furthermore differences in fractionation with temperature relate to differences in the specific temperature response to internal enzyme kinetics as well as cellular properties and corresponding exchange rates of sulfate in and out of the cell. Canfield et al. (2006) found in contrast to earlier belief high fractionations in the low and high temperature range and the lowest fractionations in the intermediate temperature range.

The reaction chain during anaerobic sulfate reduction has been described in detail by Goldhaber and Kaplan (1974). In general, the rate-limiting step is the breaking of the first S-O bond, namely the reduction of sulfate to sulfite. Pure cultures of sulfate reducing bacteria produce sulfide depleted in ^{34}S by 4–46‰ (Harrison and Thode 1957a, b; Kemp and Thode 1968; McCready et al. 1974; McCready 1975; Bolliger et al. 2001). More recently, sulfur isotope fractionations have been determined from natural populations covering a wide spectrum of environments (from rapidly metabolizing microbial mats to slowly metabolizing coastal sediments; Habicht and Canfield 1997, 2001; Canfield 2001a).

In marine coastal sediments typically 90% of the sulfide produced during sulfate reduction is reoxidized (Canfield and Teske 1996). The pathways of sulfide oxidation are poorly known but include oxidation to sulfate, elemental sulfur and other intermediate compounds. Systematic studies of sulfur isotope fractionations during sulfide oxidation are still needed, the few available data suggest that biologically mediated oxidation of sulfide to elemental sulfur and sulfate lead to only minimal isotope fractionation.

Naturally occurring sulfides in sediments and euxinic waters are commonly depleted in ^{34}S by up to 70‰ (Jørgensen et al. 2004), far beyond the apparent capabilities of sulfate reducing bacteria. As has been shown above, most of the sulfide produced by sulfate reduction in sediments is reoxidized, often via compounds in which sulfur has intermediate oxidation states that do not accumulate, but

are readily transformed and which can be disproportionated by bacteria. Canfield and Thamdrup (1994) suggested that through a repeated cycle of sulfide oxidation to elemental sulfur and subsequent disproportionation, bacteria can generate the large ^{34}S depletion typical of many marine sulfides. Thus the oxidative part of the sulfur cycle may create circumstances by which sulfides become more depleted in ^{34}S than would be possible with sulfate-reducing bacteria alone.

However, in contrast to microbiological experiments and near-surface studies, modelling of sulfate reduction in pore water profiles within the ODP program has demonstrated that natural populations are able to fractionate S-isotopes by up to more than 70‰ (Wortmann et al. 2001; Rudnicki et al. 2001). Brunner et al. (2005) suggested that S isotope fractionations of around -70‰ might occur under hyper-sulfidic, substrate-limited, but nonlimited supply of sulfate, conditions without the need of alternate pathways involving the oxidative sulfur cycle.

Another factor that is of great importance for the observed sulfur isotope variations of natural sulfides is whether sulfate reduction takes place in an open or closed system. An “open” system has an infinite reservoir of sulfate in which continuous removal from the source produces no detectable loss of material. Typical examples are the Black Sea and local oceanic deeps. In such cases, H_2S is extremely depleted in ^{34}S while consumption and change in ^{34}S remain negligible for the sulfate. In a “closed” system, the preferential loss of the lighter isotope from the reservoir has a feedback on the isotopic composition of the unreacted source material. The changes in the ^{34}S -content of residual sulfate and of the H_2S are modeled in Fig. 2.21, which shows that $\delta^{34}\text{S}$ -values of the residual sulfate steadily increase with sulfate consumption (a linear relationship on the log-normal plot). The curve for the derivative H_2S is parallel to the sulfate curve at a distance which depends on the magnitude of

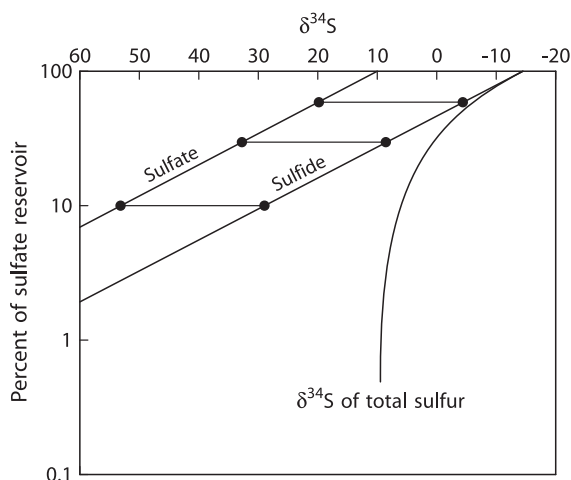


Fig. 2.21 Rayleigh plot for sulphur isotopic fractionations during the reduction of sulfate in a closed system. Assumed fractionation factor. 1.025, assumed starting composition of initial sulfate: +10‰

the fractionation factor. As shown in Fig. 2.21, H_2S may become isotopically heavier than the original sulfate when about 2/3 of the reservoir has been consumed. The $\delta^{34}\text{S}$ -curve for “total” sulfide asymptotically approaches the initial value of the original sulfate. It should be noted, however, that apparent “closed-system” behavior of covarying sulfate and sulfide $\delta^{34}\text{S}$ -values might be also explained by “open-system” differential diffusion of the different sulfur isotope species (Jørgensen et al. 2004).

In recent years additional informations on sulfur isotope fractionation mechanisms have been obtained from the analysis of the additional isotopes ^{33}S and ^{36}S (Farquhar et al. 2003; Johnston et al. 2005; Ono et al. 2006, 2007). For long it was thought $\delta^{33}\text{S}$ and $\delta^{36}\text{S}$ values carry no additional information, because sulfur isotope fractionations follow strictly mass-dependent fractionation laws. By studying all sulfur isotopes with very high precision these authors could demonstrate that bacterial sulfate reduction follows a mass-dependent relationship that is slightly different from that expected by equilibrium fractionations. On plots $\Delta^{33}\text{S}$ vs $\delta^{34}\text{S}$ mixing of two sulfur reservoirs is non-linear in these coordinates (Young et al. 2002). As a result samples with the same $\delta^{34}\text{S}$ -value can have different $\Delta^{33}\text{S}$ and $\Delta^{36}\text{S}$ values. This opens the possibility to distinguish between different fractionation mechanisms and biosynthetic pathways (Ono et al. 2006, 2007). For instance, bacterial sulfate reduction shows slightly different fractionation relationships compared to sulfur disproportionation reactions (Johnston et al. 2005). Thus multiple sulfur isotope analyses might have great potential in identifying the presence or absence of specific metabolisms in modern environment or to have a fingerprint when a particular sulfur metabolism shows up in the geologic record.

Finally it should be mentioned that sulfate is labeled with two biogeochemical isotope systems, sulfur and oxygen. Coupled isotope fractionations of both sulfur and oxygen isotopes have been observed in experiments (Mizutani and Rafter 1973; Fritz et al. 1989; Böttcher et al. 2001) and in naturally occurring sediments (Ku et al. 1999; Aharon and Fu 2000; Wortmann et al. 2001). Brunner et al. (2005) argued that characteristic $\delta^{34}\text{S}$ - $\delta^{18}\text{O}$ fractionation slopes do not exist, but depend on cell-specific reduction rates and oxygen isotope exchange rates. Despite the extremely slow oxygen isotope exchange of sulfate with ambient water, $\delta^{18}\text{O}$ in sulfate obviously depend on the $\delta^{18}\text{O}$ of water via an exchange of sulfite with water.

2.9.2.2 Thermochemical Reduction of Sulfate

In contrast to bacterial reduction thermochemical sulfate reduction is an abiotic process with sulfate being reduced to sulfide under the influence of heat rather than bacteria (Trudinger et al. 1985; Krouse et al. 1988). The crucial question, which has been the subject of a controversial debate, is whether thermochemical sulfate reduction can proceed at temperatures as low as about 100°C , just above the limit of microbiological reduction (Trudinger et al. 1985). There is increasing evidence from natural occurrences that the reduction of aqueous sulfates by organic compounds can occur at temperatures as low as 100°C , given enough time for the reduction to proceed (Krouse et al. 1988; Machel et al. 1995). S isotope fractionations during

thermochemical reduction generally should be smaller than during bacterial sulfate reduction. However, experiments by Kiyosu and Krouse (1990) have indicated S-isotope fractionations of 10 to 20‰ in the temperature range of 200 to 100°C.

To summarize, bacterial sulfate reduction is characterized by large and heterogeneous ^{34}S -depletions over very small spatial scales, whereas thermogenic sulfate reduction leads to smaller and “more homogeneous” ^{34}S -depletions.

2.9.2.3 Isotope Exchange Reactions

There have been a number of theoretical and experimental determinations of sulfur isotope fractionations between coexisting sulfide phases as a function of temperature. Theoretical studies of fractionations among sulfides have been undertaken by Sakai (1968) and Bachinski (1969), who reported the reduced partition function ratios and the bond strength of sulfide minerals and described the relationship of these parameters to isotope fractionation. In a manner similar to that for oxygen in silicates, there is a relative ordering of ^{34}S -enrichment among coexisting sulfide minerals (Table 2.9). Considering the three most common sulfides (pyrite, sphalerite and galena) under conditions of isotope equilibrium pyrite is always the most ^{34}S enriched mineral and galena the most ^{34}S depleted, sphalerite displays an intermediate enrichment in ^{34}S .

The experimental determinations of sulfur isotope fractionations between various sulfides do not exhibit good agreement. The most suitable mineral pair for temperature determination is the sphalerite–galena pair. Rye (1974) has argued that the Czamanske and Rye (1974) fractionation curve gives the best agreement with filling temperatures of fluid inclusions over the temperature range from 370 to 125°C. By contrast, pyrite – galena pairs do not appear to be suitable for a temperature determination, because pyrite tends to precipitate over larger intervals of ore deposition than galena, implying that these two minerals may frequently not be contemporaneous. The equilibrium isotope fractionations for other sulfide pairs are generally so small that they are not useful as geothermometers. Ohmoto and Rye (1979) critically examined the available experimental data and presented a

Table 2.9 Equilibrium isotope fractionation factors of sulfides with respect to H_2S . The temperature dependence is given by A/T^2 (after Ohmoto and Rye 1979)

Mineral	Chemical composition	A
Pyrite	FeS_2	0.40
Sphalerite	ZnS	0.10
Pyrrhotite	FeS	0.10
Chalcopyrite	CuFeS_2	−0.05
Covellite	CuS	−0.40
Galena	PbS	−0.63
Chalcosite	Cu_2S	−0.75
Argentite	Ag_2S	−0.80

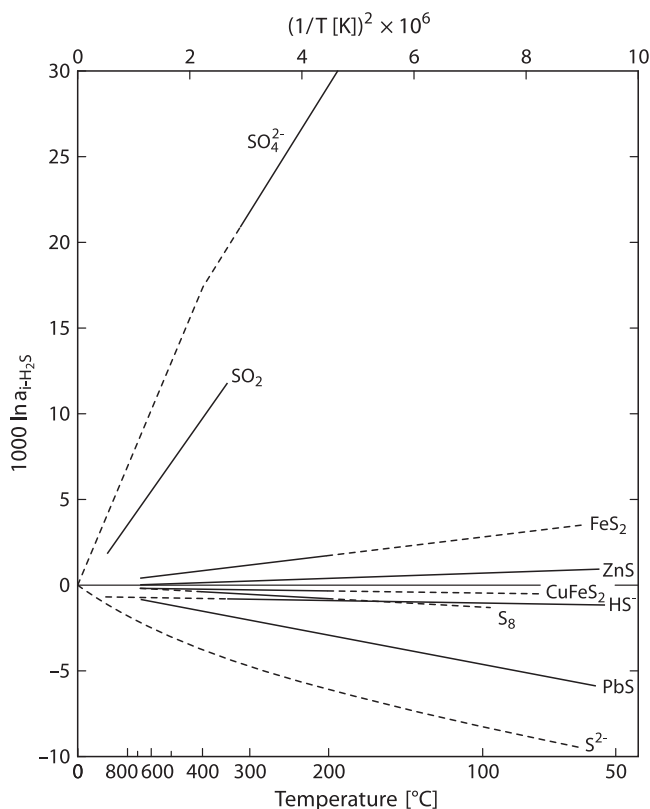


Fig. 2.22 Equilibrium fractionations among sulphur compounds relative to H_2S (solid lines experimentally determined, dashed lines extrapolated or theoretically calculated (after Ohmoto and Rye, 1979))

summary of what they believe to be the best S-isotope fractionation data. These S-isotope fractionations relative to H_2S are shown in Fig. 2.22.

Sulfur isotope temperatures from ore deposits often have been controversial; one of the reasons are strong ^{34}S zonations in sulfide minerals that have been observed by laser probe and ion probe measurements (McKibben and Riciputi 1998).

2.10 Chlorine

Chlorine has two stable isotopes with the following abundances (Coplen et al. 2002):

^{35}Cl 75.78%

^{37}Cl 24.22%

Natural isotope variations in chlorine isotope ratios might be expected due to both the mass difference between ^{35}Cl and ^{37}Cl as well as to variations in coordination of chlorine in the vapor, aqueous and solid phases. Schauble et al. (2003) calculated equilibrium fractionation factors for some geochemically important species. They showed that the magnitude of fractionations systematically varies with the oxidation state of Cl, but also depends on the oxidation state of elements to which Cl is bound with greater fractionations for 2+ cations than for 1+ cations. Silicates are predicted to be enriched compared to coexisting brines and organic molecules are enriched to dissolved Cl^- .

2.10.1 Methods

Measurements of Cl-isotope abundances have been made by different techniques. The first measurements by Hoering and Parker (1961) used gaseous chlorine in the form of HCl and the 81 samples measured exhibited no significant variations relative to the standard ocean chloride. In the early eighties a new technique has been developed by Kaufmann et al. (1984), that uses methylchloride (CH_3Cl). The chloride-containing sample is precipitated as AgCl, reacted with excess methyl iodide, and separated by gas chromatography. The total analytical precision reported is near $\pm 0.1\%$ (Long et al. 1993; Eggenkamp 1994; Sharp et al. 2007). The technique requires relatively large quantities of chlorine (>1 mg), which precludes the analysis of materials with low chlorine concentrations or which are limited in supply. Magenheimer et al. (1994) described a method involving the thermal ionization of Cs_2Cl^+ , which, as argued by Sharp et al. (2007), is very sensitive to analytical artefacts and therefore might lead to erroneous results. δ -values are generally given relative to seawater chloride termed SMOC (Standard Mean Ocean Chloride).

2.10.2 Characteristic Features of Cl Isotope Geochemistry

Chlorine is the major anion in surface- and mantle-derived fluids. It is the most abundant anion in hydrothermal solutions and is the dominant metal complexing agent in ore forming environments (Banks et al. 2000). Despite its variable occurrence, chlorine isotope variations in natural waters commonly are small and close to the chlorine isotope composition of the ocean. This is also true for chlorine from fluid inclusions in hydrothermal minerals which indicate no significant differences between different types of ore deposits such as Mississippi-Valley and Porphyry Copper type deposits (Eastoe et al. 1989; Eastoe and Guilbert 1992).

Relatively large isotopic differences have been found in slow flowing groundwater, where Cl-isotope fractionation is attributed to a diffusion process (Kaufmann et al. 1984, 1986; Desaulniers et al. 1986). ^{37}Cl depletions detected in some pore waters have been attributed to processes such as ion filtration, alteration and dehydration

reactions and clay mineral formation (Long et al. 1993; Eggenkamp 1994; Eastoe et al. 2001; Hesse et al. 2006). A pronounced downward depletion of $\delta^{37}\text{Cl}$ -values to -4‰ has been reported by Hesse et al. (2006). Even lower $\delta^{37}\text{Cl}$ -values have been reported in pore waters from subduction-zone environments (Ransom et al. 1995; Spivack et al. 2002). The downward depletion trend might be explained by mixing of two fluids: shallow ocean water with a deep low ^{37}Cl fluid of unknown origin.

Controversial results have been reported for chlorine isotopes in mantle-derived rocks. According to Magenheimer et al. (1995) $\delta^{37}\text{Cl}$ -values for MORB glasses show a surprisingly large range. As postulated by Magenheimer et al. (1995), characteristic differences between mantle and crustal chlorine can be used as indicators of the source of volatiles in chlorine-rich mafic magmas, such as the Bushveld and Stillwater complexes (Boudreau et al. 1997; Willmore et al. 2002). For the Stillwater Complex chlorine isotopes are consistent with an influence of crustal derived fluid, whereas for the Bushveld Complex chlorine isotopes indicate a mantle-derived source. A similar approach has been taken by Markl et al. (1997) to trace the origin of chlorine in the lower crust. Since $\delta^{37}\text{Cl}$ values of granulite facies rocks cluster around ocean water composition, Markl et al. (1997) concluded that chlorine in the lower crust is derived from the upper crust and therefore does not reflect degassing of the mantle.

Recently Sharp et al. (2007) have questioned the findings of Magenheimer et al. (1995). Sharp et al. (2007) found that the large differences between mantle and crustal material do not exist and that the mantle and the crust have very similar isotopic composition. A possible explanation for this apparent discrepancy might be related to analytical artifacts of the TIMS technique (Sharp et al. 2007). Bonifacie et al. (2008) also observed small Cl-isotope variations only in mantle derived rocks. They demonstrated that $\delta^{37}\text{Cl}$ values correlate with chlorine concentrations: Cl-poor basalts have low $\delta^{37}\text{Cl}$ values and represent the composition of uncontaminated mantle derived magmas, whereas Cl-rich basalts are enriched in ^{37}Cl and are contaminated by Cl-rich material such as ocean water.

Volcanic gases and associated hydrothermal waters have a large range in $\delta^{37}\text{Cl}$ -values from -2 to $+12\text{‰}$ (Barnes et al. 2006). To evaluate chlorine isotope fractionations in volcanic systems, HCl liquid-vapor experiments performed by Sharp (2006) yield large isotope fractionations of dilute HCl at 100°C . These results are in contrast to liquid-vapor experiments by Liebscher et al. (2006) observing very little fractionation at $400 - 450^\circ\text{C}$. Clearly more data are needed to resolve these discrepancies.

2.10.3 Chlorine Isotopes in the Environment

Chlorine isotope studies have been applied to understand the environmental chemistry of anthropogenic organic compounds, such as chlorinated organic solvents or biphenyls. The primary goal of such studies is to identify and quantify sources and

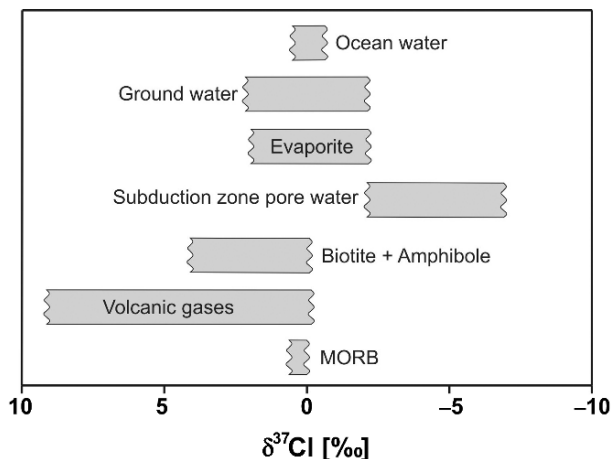


Fig. 2.23 $\delta^{37}\text{Cl}$ values in geologically important reservoirs

biodegradation processes in the environment. To do this successfully chlorine isotope values should differ among compounds and manufacturers. The range of reported $\delta^{37}\text{Cl}$ -values is from about -5 to $+6\text{‰}$ with distinct signatures from different suppliers (Van Warmerdam et al. 1995; Jendrzewski et al. 2001).

Perchlorate is another anthropogenic compound, which may contaminate surface and ground waters. The occurrence of natural perchlorate is limited to extremely dry environments, such as the Atacama desert. Large kinetic isotope effects during microbial reduction of perchlorate have been observed by Sturchio et al. (2003) and Ader et al. (2008), which may be used to document in-situ bioremediation.

A summary of the observed natural chlorine isotope variations is presented in Fig. 2.23. Ransom et al. (1995) gave a natural variation range in chlorine isotope composition of about 15‰ with subduction zone pore waters having $\delta^{37}\text{Cl}$ values as low as -8‰ whereas minerals in which Cl substitutes OH have $\delta^{37}\text{Cl}$ values as high as 7‰ .

2.11 Calcium

Calcium plays an essential role in biological processes (calcification of organisms, formation of bones etc.). Calcium has six stable isotopes in the mass range of 40 to 48 with the following abundances (Rosman and Taylor 1998)

- ^{40}Ca : 96.94%
- ^{42}Ca : 0.647%
- ^{43}Ca : 0.135%
- ^{44}Ca : 2.08%
- ^{46}Ca : 0.004%
- ^{48}Ca : 0.187%

Its wide natural distribution and the large relative mass difference suggest a large isotope fractionation, which might be caused by mass-dependent fractionation processes and by radiogenic growth (radioactive decay of ^{40}K), the latter not being discussed here. Early studies on natural isotope variations found no differences or ambiguous results. By using a double-spike technique and by using a mass-dependent law for correction of instrumental mass fractionation Russell et al. (1978) were the first to demonstrate that differences in the $^{44}\text{Ca}/^{40}\text{Ca}$ ratio are clearly resolvable to a level of 0.5‰. More recent investigations by Skulan et al. (1997) and by Zhu and MacDougall (1998) have improved the precision to about 0.1–0.15‰. These latter authors observed Ca-isotope variations – given as $\delta^{44}\text{Ca}$ -values – of about 5‰ (see also the review by DePaolo 2004). Comparing data from different laboratories, complications may arise from the use of different δ -definitions and from the use of different standards. By initiating a laboratory exchange of internal standards Eisenhauer et al. (2004) have suggested to use NIST SRM 915a as international standard.

New insights on biomineralization may be revealed by measuring Ca isotope variations in shell secreting organisms (e.g. Griffith et al. 2008). Two factors influence the Ca isotope composition of shells: (1) the chemistry of the solution, in which the organisms live and (2) the process by which Ca is precipitated.

The magnitude of Ca isotope fractionation during carbonate precipitation as well as the mechanism – either isotope equilibrium or kinetic effects – remain a matter of debate. Studies by Nägler et al. (2000), Gussone et al. (2005) and Hippler et al. (2006) reported temperature dependent Ca isotope fractionations precipitated in natural environments or under cultured laboratory conditions with a slope of about 0.02‰ per °C. The slope is identical for aragonite and calcite with an offset of about 0.6‰: aragonite being isotopically lighter ($\delta^{44}\text{Ca} \approx 0.4‰$) than calcite ($\delta^{44}\text{Ca} \approx 1.0‰$). An important question is whether the observed temperature-dependent fractionation results solely from temperature or whether it is influenced by temperature related changes in growth and calcification rates (Langer et al. 2007). And as pointed out by Gussone et al. (2006) similar temperature dependencies do not necessarily imply the same fractionation mechanism. Temperature dependent fractionations; however, have not been found in all shell secreting organisms (Lemarchand et al. 2004; Sime et al. 2005). Sime et al. (2005) analyzed 12 species of foraminifera and found negligible temperature dependence for all 12 species. Thus, no consensus on temperature controlled Ca isotope fractionations has been reached (Griffith et al. 2008).

Marine biogenic carbonates are isotopically depleted in ^{44}Ca relative to present-day seawater (Skulan et al. 1997; Zhu and MacDougall 1998). Zhu and MacDougall have made the first attempt to investigate the global Ca cycle. They found a homogeneous isotope composition of the ocean, but distinct isotope differences of the sources and sinks and suggested that the ocean is not in steady state. Since then several other studies have investigated secular changes in the Ca isotope composition of the ocean: De La Rocha and de Paolo (2000) and Fantle and de Paolo (2005) for the Neogene, Steuber and Buhl (2006) for the Cretaceous; Farkas et al. (2007). for the late Mesozoic; and Kasemann et al. (2005) for the Neoproterozoic. Model

simulations of the Ca cycle by Farkas et al. (2007) indicated that the observed Ca isotope variations can be produced by variable Ca input fluxes to the oceans. However, since the isotope effects that control the Ca isotope composition of marine carbonates are not well understood, any clear indication of secular changes in the Ca isotope composition of ocean waters must remain subject of further debate.

2.12 Chromium

Chromium has 4 stable isotopes with the following abundances (Rosman and Taylor 1998)

^{50}Cr 4.35%

^{52}Cr 83.79%

^{53}Cr 9.50%

^{54}Cr 2.36%

Chromium exists in two oxidation states, Cr(III), as a cation Cr^{3+} and Cr(VI), as an oxyanion (CrO_4^{2-} or HCrO_4^-) having different chemical behaviors: Cr^{3+} is the dominant form in most minerals and in water under reducing conditions, whereas Cr(VI) is stable under oxidizing conditions. These properties make Cr isotope investigations suitable to detect and quantify redox changes in different geochemical reservoirs.

Schoenberg et al. (2008) presented the first set of Cr isotope data for rocks and Cr(II) rich ores. Mantle derived rocks and chromite ores from layered intrusions have a uniform $^{53}\text{Cr}/^{52}\text{Cr}$ isotope ratio very close to the certified Cr standard NIST SRM 979. The Cr isotope composition of hydrothermal lead chromates is substantially heavier ($\delta^{53}\text{Cr}$ from 0.6 to 1.0‰) than the rocks from which the chromium was leached.

Chromium is a common anthropogenic contaminant in surface waters, therefore Cr isotope fractionations are of potential interest in tracking Cr^{6+} pollution in groundwaters. Ellis et al. (2002, 2004) and Izbicki et al. (2008) analyzed groundwater samples from contaminated sites and observed an increase in $^{53}\text{Cr}/^{52}\text{Cr}$ ratios up to 6‰ during the reduction of chromate. Equilibrium fractionations between Cr(VI) and Cr(III) have been estimated by Schauble et al. (2002), who predicted Cr isotope fractionations $>1‰$ between Cr species with different oxidation states.

2.13 Iron

Iron has 4 stable isotopes with the following abundances (Beard and Johnson 1999)

^{54}Fe 5.84%

^{56}Fe 91.76%

^{57}Fe 2.12%

^{58}Fe 0.28%

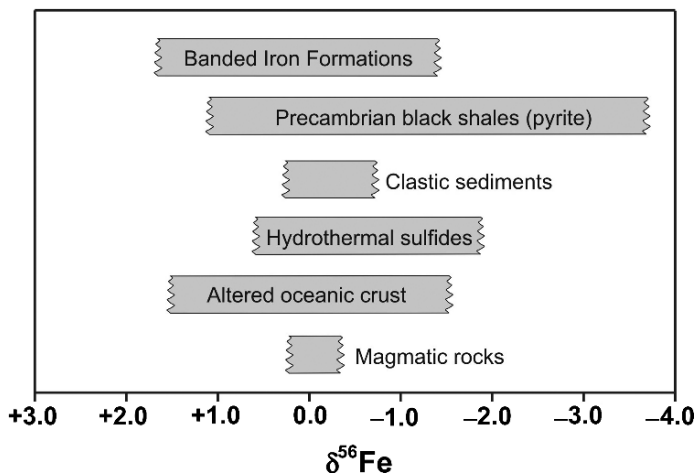


Fig. 2.24 $\delta^{56}\text{Fe}$ ranges in some important iron reservoirs

Iron is the third most abundant element that participates in a wide range of biotically and abiotically-controlled redox processes in different geochemical low- and high-temperature environments. Iron has a variety of important bonding partners and ligands, forming sulfide, oxide and silicate minerals as well as complexes with water. As is well known bacteria can use Fe during both dissimilatory and assimilatory redox processes. Because of its high abundance and its prominent role in high and low temperature processes, isotope studies of iron have received the most attention of the transition elements. Since the first investigations on Fe isotope variations by Beard and Johnson (1999), the number of studies on Fe isotope variations have increased exponentially. Recent reviews on Fe-isotope geochemistry have been given by Anbar (2004a), Beard and Johnson (2004), Johnson and Beard (2006), Dauphas and Rouxel (2006) and Anbar and Rouxel (2007). Figure 2.24 summarizes Fe-isotope variations in important geological reservoirs.

Literature data have been presented either in the form of $^{57}\text{Fe}/^{54}\text{Fe}$ or as $^{56}\text{Fe}/^{54}\text{Fe}$ ratios. In the following all data are given as $^{56}\text{Fe}/^{54}\text{Fe}$ ratios or as $\delta^{56}\text{Fe}$ values. $\delta^{57}\text{Fe}$ values would be 1.5 times greater than $\delta^{56}\text{Fe}$ values, because only mass-dependent fractionations are expected. Fe isotope analysis is highly challenging because of interferences from $^{40}\text{Ar}^{14}\text{N}^+$, $^{40}\text{Ar}^{16}\text{O}^+$ and $^{40}\text{Ar}^{16}\text{OH}^+$ at masses 54, 56 and 57 respectively. Nevertheless δ -values can be measured routinely with a precision of $\pm 0.05\text{‰}$.

Theoretical studies by Polyakov (1997), Polyakov et al. (2007) and Schauble et al. (2001) predicted Fe isotope fractionations of several ‰ between various iron oxides, carbonates and sulfides from spectroscopic data, even at high temperatures. $^{56}\text{Fe}/^{54}\text{Fe}$ ratios will be usually higher in Fe^{3+} compounds than in Fe^{2+} bearing species. First experimental studies at magmatic temperatures were conducted by Schüßler et al. (2007) for equilibrium isotope fractionations between iron sulfide

(pyrrhotite) and silicate melt and by Shahar et al. (2008) for those between fayalite and magnetite, demonstrating that Fe isotope fractionations are relatively large at magmatic temperatures and can be used as a geothermometer. At low temperatures, Johnson et al. (2002) presented experimental evidence for equilibrium fractionations between Fe^{3+} and Fe^{2+} in aqueous solutions. They observed a 2.75‰ enrichment in Fe^{3+} relative to Fe^{2+} at 25°C which is about half of that predicted by Schauble et al. (2001). While it is conceivable that Fe isotope equilibrium can be reached at high temperatures, indications for equilibrium fractionations are less straightforward at much lower temperatures. Therefore kinetic fractionations might dominate Fe isotope fractionations at low temperatures.

Igneous rocks exhibit only small variations in Fe isotope compositions (Zhu et al. 2002; Beard and Johnson 2004; Poitrasson et al. 2004; Williams et al. 2005; Weyer et al. 2005). Weyer et al. (2005) found that the Fe isotope composition in mantle peridotites is slightly lower than in basalts. As suggested by Williams et al. (2005) the relative incompatibility of ferric iron during melting might incorporate heavy iron into the melt. During magmatic differentiation the Fe isotope composition remains more or less constant except in the very SiO_2 -rich differentiates (Beard and Johnson 2004; Poitrasson and Freydier 2005). A possible mechanism is removal of isotopically ^{56}Fe depleted titanomagnetite (Schüßler et al. 2008).

Under low-temperature conditions the observed natural Fe isotope variations of around 4‰ have been attributed to a large number of processes, which can be divided into inorganic reactions and into processes initiated by micro-organisms. Up to 1‰ fractionation can result from precipitation of Fe-containing minerals (oxides, carbonates, sulfides) (Anbar and Rouxel 2007). Larger Fe isotope fractionations occur during biogeochemical redox processes, which include dissimilatory Fe(III) reduction (Beard et al. 1999; Icopini et al. 2004; Crosby et al. 2007), anaerobic photosynthetic Fe(II) oxidation (Croal et al. 2004), abiotic Fe (II) oxidation (Bullen et al. 2001) and sorption of aqueous Fe(II) on Fe(III) hydroxides (Balci et al. 2006). Controversy still exists whether the iron isotope variations observed are controlled by kinetic/equilibrium factors or by abiological/microbiological fractionations. This complicates the ability to use iron isotopes to identify microbiological processing in the rock record (Balci et al. 2006). However, as demonstrated by Johnson et al. (2008) microbiological reduction of Fe^{3+} produces much larger quantities of iron with distinct $\delta^{56}\text{Fe}$ values than abiological processes.

The bulk continental crust has $\delta^{56}\text{Fe}$ values close to zero. Clastic sediments generally retain the zero ‰ value. Because of its very low concentration in the ocean, the Fe isotope composition of ocean water so far has not been determined, which complicates a quantification of the modern Fe isotope cycle. Hydrothermal fluids at mid-ocean ridges and river waters have $\delta^{56}\text{Fe}$ values between 0 and -1‰ (Fantle and dePaolo 2004; Bergquist and Boyle 2006; Severmann et al. 2004), whereas fluids in diagenetic systems show a significantly larger spread with a preferential depletion in ^{56}Fe (Severmann et al. 2006). Thus, most iron isotope variations are produced by diagenetic processes that reflect the interaction between Fe^{3+} and Fe^{2+} during bacterial iron and sulfate reduction. Processes dominated by sulfide formation during sulfate reduction produce high $\delta^{56}\text{Fe}$ values for porewaters, whereas the

opposite occurs when dissimilatory iron reduction is the major pathway (Severmann et al. 2006).

Especially large iron isotope fractionations have been found in Proterozoic and Archean sedimentary rocks with lithologies ranging from oxide to carbonate in banded iron formations (BIFs) and pyrite in shales (Rouxel et al. 2005; Yamaguchi et al. 2005). In particular BIFs have been investigated to reconstruct Fe cycling through Archean oceans and the rise of $O_{2(atm)}$ during the Proterozoic (see discussion under 3.8.4 and Fig. 3.28). The pattern shown in Fig. 3.28 distinguishes three stages of Fe isotope evolution, which might reflect redox changes in the Fe cycle (Rouxel et al. 2005). The oldest samples (stage 1) are characterized by depleted $\delta^{56}Fe$ values, whereas younger samples in stage 2 are characterized by enriched $\delta^{56}Fe$ values. Interplays of the Fe-cycle with the C- and S-record might reflect changing microbial metabolisms during the Earth's history (Johnson et al. 2008).

2.14 Copper

Copper has two stable isotopes

^{63}Cu 69.1%

^{65}Cu 30.9%.

Copper occurs in two oxidation states, Cu^+ and Cu^{++} and rarely in the form of elemental copper. The major Cu-containing minerals are sulfides (chalcopyrite, bornite, chalcosite and others), and, under oxidizing conditions, secondary copper minerals in the form of oxides and carbonates. Copper is a nutrient element, although toxic for all aquatic photosynthetic microorganisms. Copper may form a great variety of complexes with very different coordinations such as square, trigonal and tetragonal complexes. These properties are ideal prerequisites for relatively large isotope fractionations.

Early work of Shields et al. (1965) has indicated a total variation of $\sim 12\text{‰}$ with the largest variations in low temperature secondary minerals. Somewhat smaller differences, but still in the range of 7 to 9‰, have been observed by Maréchal et al. (1999), Maréchal and Albarede (2002), Zhu et al. (2002), Ruiz et al. (2002), which are larger than for Fe. Nevertheless most samples so far analyzed vary between $\delta^{65}Cu$ values from +1 to -1‰ .

Experimental investigations have demonstrated that redox reactions between CuI and CuII species are the principal process that fractionates Cu isotopes in natural systems (Ehrlich et al. 2004; Zhu et al. 2002). Precipitated CuI species are 3 to 5‰ lighter than dissolved CuII species during CuII reduction. Pokrovsky et al. (2008) observed a change in sign of Cu isotope fractionations during adsorption experiments from aqueous solutions depending on the kind of surface, either organic or inorganic: on biological cell surfaces a depletion of ^{65}Cu , whereas an enrichment of ^{65}Cu on oxy(hydr)oxide surface is observed. Although little is known about the Cu isotope composition of ocean water, Zhu et al. (2002) suggested that Cu isotopes

may be a tracer of Cu biochemical cycling. The latter authors reported Cu isotope fractionations of 1.5‰ during biological uptake.

Recent studies of Cu isotope variations have concentrated on Cu isotope fractionations during ore formation (Larson et al. 2003; Rouxel et al. 2004; Mathur et al. 2005; Markl et al. 2006a). The magnitude of isotope fractionation in copper sulfides increases with secondary alteration and reworking processes. Investigations by Markl et al. (2006) on primary and secondary copper minerals from hydrothermal veins have confirmed this conclusion. They showed that hydrothermal processes do not lead to significant Cu isotope variations, but instead, low temperature redox processes are the main cause of isotope fractionations. Thus copper isotope ratios may be used to decipher details of natural redox processes, but cannot be used as reliable fingerprints for the source of copper – as suggested by Graham et al. (2004) – because the variation caused by redox processes within a single deposit is usually much larger than the inter-deposit variation.

2.15 Zinc

Zinc has 5 stable isotopes of mass 64, 66, 67, 68 and 70 with the following abundances:

^{64}Zn 48.63,
 ^{66}Zn 27.90,
 ^{67}Zn 4.10,
 ^{68}Zn 18.75,
 ^{70}Zn 0.62.

Zinc is an essential biological nutrient in the ocean where the concentration of Zn is controlled by phytoplankton uptake and remineralization. Zn is incorporated into carbonate shells and diatoms, therefore, Zn isotopes may have great potential for tracing nutrient cycling in seawater. John et al. (2007a) measured the isotope fractionation of Zn during uptake by diatoms and demonstrated that Zn isotope fractionations are related to the extent of biological Zn uptake. In a depth profile of the upper 400 m of Pacific seawater, Bermin et al. (2006) observed small isotope variations which they interpreted as being due to biological recycling. Surface waters have a lighter $\delta^{66}\text{Zn}$ signature than deeper waters suggesting that absorption of Zn on particle surfaces carries Zn out of surface waters (John et al. 2007a). Pichat et al. (2003) suggested that variations in Zn isotopes in marine carbonates over the last 175 kyr reflect changes in upwelling and nutrient availability. Although it has been assumed that there is negligible fractionation between Zn in seawater and precipitated minerals, biological usage and adsorption onto particles are likely to cause isotope fractionations (Gelabert et al. 2006).

Measurements of the $^{66}\text{Zn}/^{64}\text{Zn}$ ratio in ores, sediments and biological materials have so far yielded a small variation of about 1‰ (Maréchal et al. 1999, 2000; Maréchal and Albarede 2002 and others). One of the main reasons for this small

variability appears to be that Zn does not participate in any redox reaction, it always occurs in the divalent state. Recently Wilkinson et al. (2005) extended the range of Zn isotope variations to $\sim 1.5\text{‰}$ by analyzing sphalerites from one ore deposit. They interpreted the variations by postulating kinetic fractionations during rapid sphalerite precipitation. John et al. (2008) have found relatively large Zn isotope fractionation in hydrothermal fluids and suggested that Zn sulfide precipitation is an important factor in causing $\delta^{66}\text{Zn}$ variations. By analyzing common anthropogenic products in the environment, John et al. (2007b) showed that $\delta^{66}\text{Zn}$ values of industrial products are smaller than of Zn ores demonstrating Zn isotope homogenization during processing and ore purification.

2.16 Germanium

Because of nearly identical ionic radii, Ge usually replaces Si in minerals, with average concentrations around 1 ppm in the earth's crust. Thus Ge and Si have similar chemistries, which might indicate that both elements show similarities in their isotope fractionations.

Ge has five stable isotopes with the following abundances (Rosman and Taylor 1998):

^{70}Ge 20.84%

^{72}Ge 27.54%

^{73}Ge 7.73%

^{74}Ge 36.28%

^{76}Ge 7.61%

Early investigations using the TIMS method were limited to an uncertainty of several ‰. Over the past few years advances have been made with the MC-ICP-MS technique with a long term external reproducibility of 0.2–0.4‰ (Rouxel et al. 2006; Siebert et al. 2006a).

Based on a few measurements of basalts and granites Rouxel et al. (2006) concluded that the bulk silicate earth has a homogeneous isotope composition. However, chemical sediments like sponges and authigenic glauconites are enriched in $\delta^{74}\text{Ge}$ by about 2‰. This suggests that seawater – similar to silicon – is isotopically enriched in ^{74}Ge relative to the bulk earth. Ge isotopes might offer new insights into the biogeochemistry of the past and present ocean, but more data are needed.

2.17 Selenium

Because selenium to some extent is chemically similar to sulfur, one might expect to find some analogous fractionations of selenium isotopes in nature. Six stable selenium isotopes are known with the following abundances (Coplen et al. 2002)

^{74}Se 0.89%
 ^{76}Se 9.37%
 ^{77}Se 7.63%
 ^{78}Se 23.77%
 ^{80}Se 49.61%
 ^{82}Se 8.73%

Interest in selenium isotope studies has grown in recent years, since selenium is both a nutrient and a toxicant and may reach significant concentrations in soils and in watersheds. Starting with work by Krouse and Thode (1962) the SeF_6 gas technique used by the early workers required relatively large quantities of Se, limiting the applications of selenium isotopes. Johnson et al. (1999) developed a double-spike solid-source technique (spike ^{74}Se and ^{82}Se , measure $^{80}\text{Se}/^{76}\text{Se}$) that corrects for fractionations during sample preparation and mass spectrometry, yielding an overall reproducibility of $\pm 0.2\%$. This technique brings sample requirements down to sub-microgram levels. Even lower Se amounts (10 ng) are required for measurements with the MC-ICP-MS technique (Rouxel et al. 2002).

Reduction of selenium oxyanions by bacteria is an important process in the geochemical cycle of selenium. Selenium reduction proceeds in three steps with Se(IV) and Se(0) species as stable intermediates (Johnson 2004). Se isotope fractionation experiments by Herbel et al. (2000) indicate about 5‰ fractionations ($^{80}\text{Se}/^{76}\text{Se}$) during selenate reduction to selenite and little or no fractionation for selenite sorption, oxidation of reduced Se in soils, or Se volatilization by algae. Johnson and Bullen (2003) investigated Se isotope fractionations induced by inorganic reduction of selenate by $\text{Fe(II)}\text{--Fe(III)}$ hydroxide sulfate (“green rust”). The overall fractionation is 7.4‰, which is larger than during bacterial selenate reduction. This indicates that the magnitude of Se isotope fractionations depends on the specific reaction mechanism. More data are needed, but selenium isotopes should be useful tracers for selenate and selenite reduction processes as well as selenium sources.

2.18 Molybdenum

Mo consists of 7 stable isotopes that have the following abundances:

^{92}Mo 15.86%,
 ^{94}Mo 9.12%,
 ^{95}Mo 15.70%,
 ^{96}Mo 16.50%,
 ^{97}Mo 9.45%,
 ^{98}Mo 23.75%
 ^{100}Mo 9.62%.

Either $^{97}\text{Mo}/^{95}\text{Mo}$ or $^{98}\text{Mo}/^{95}\text{Mo}$ ratios have been reported in the literature. Therefore care has to be taken by comparing Mo isotope values. Mo isotope data are gen-

erally given relative to laboratory standards calibrated against ocean water (Barling et al. 2001; Siebert et al. 2003).

Because Mo is a redox sensitive element that becomes enriched in reducing, organic rich sediments, Mo-isotope fractionations during redox processes might be expected (Anbar 2004b; Anbar and Rouxel 2007). In oxygenated waters insoluble MoO_4^{2-} is the dominant Mo species, which is so unreactive that Mo is the most abundant transition metal in ocean water. Mo in ocean water should have a uniform isotope composition as is expected from its long residence time in the ocean. Oxic pelagic sediments and Fe-Mn crusts or nodules are depleted in ^{98}Mo by about 3‰ relative to sea water (Barling et al. 2001; Siebert et al. 2003). A comparable fractionation has been found in pore waters (McManus et al. 2002) and in an experimental study of Mo absorption on Mn oxides (Barling and Anbar 2004). The actual fractionation mechanism is unclear, but fractionations occur in solution, where Mo is in the hexavalent state. Therefore oxidizing conditions in the marine environment are a major requirement for Mo isotope fractionations (Siebert et al. 2005).

The largest isotope effect occurs during adsorption of dissolved Mo to Mn-oxide particles, so that dissolved Mo is heavier than particle bound Mo. First observed in oxic seawater and sediments by Barling et al. (2001), Barling and Anbar (2004) have verified the fractionation effect in the laboratory. Smaller isotope fractionations occur during the reduction of Mo in suboxic environments (McManus et al. 2002, 2006; Nägler et al. 2005; Poulson et al. 2006; Siebert et al. 2003, 2006b). Observed in different sedimentary settings these effects so far have not been verified in experimental studies.

Due to the preferential extraction of ^{95}Mo from ocean water, the ocean is the heaviest Mo reservoir of all sources analyzed so far Fig. 2.24, consequently the Mo isotope composition of the ocean is sensitive to redox changes and thus can be used as a paleo-redox proxy.

Black shales that are formed in an anoxic environment such as the Black Sea have a Mo isotope composition nearly identical to ocean water (Barling et al. 2001; Arnold et al. 2004; Nägler et al. 2005). Organic carbon rich sediments formed in suboxic environments have variable $^{98}\text{Mo}/^{95}\text{Mo}$ ratios intermediate between those of ocean water and oxic sediments (Siebert et al. 2003). Thus Mo isotope values in ancient black shales can be used as a paleo-oceanographic proxy of the oxidation state of the ocean, as for example has been discussed by Arnold et al. (2004) for the Proterozoic. Figure 2.25 summarizes natural Mo isotope variations.

2.19 Mercury

The heaviest elements with observed fractionations of about 3 to 4‰ are mercury and thallium. This is surprising because isotope variations due to mass-dependent fractionations should be much smaller. Schauble (2007) demonstrated that isotope variations for the heaviest elements are controlled by nuclear volume, a fractionation effect being negligible for the light elements. Nuclear volume fractionations may

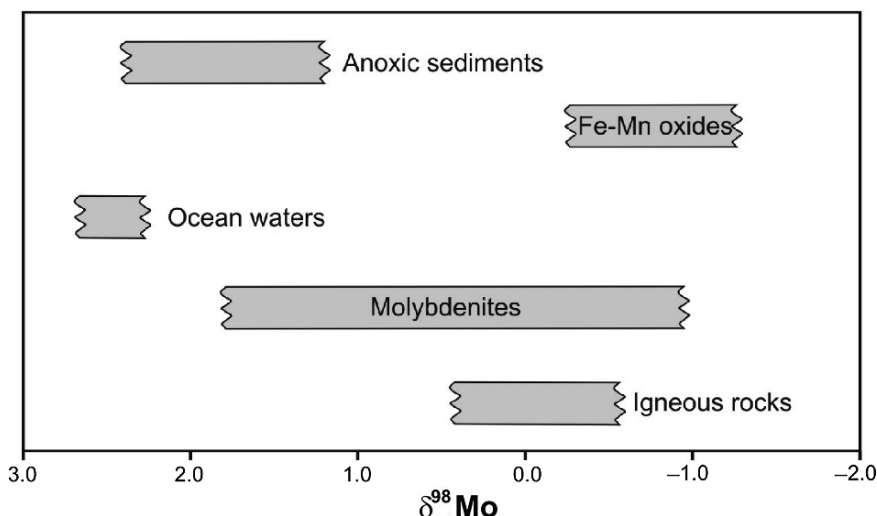


Fig. 2.25 $\delta^{97}\text{Mo}$ values in important geologic reservoirs

be about 1‰ per mass unit for Hg and Tl, declining to about 0.02‰ for sulfur. Nuclear volume fractionations also tend to enrich heavy isotopes in oxidized species (Schauble 2007).

Mercury has seven stable isotopes in the mass range from ^{196}Hg to ^{204}Hg with the following abundances (Rosman and Taylor 1998)

^{196}Hg	0.15
^{198}Hg	9.97
^{199}Hg	16.87
^{200}Hg	23.10
^{201}Hg	13.18
^{202}Hg	29.86
^{204}Hg	6.87

Due to the relative uniform isotope abundances in the mass range ^{198}Hg to ^{204}Hg , several possibilities exist for the measurement of isotope ratios, thus far δ -values are generally presented as $^{202}\text{Hg}/^{198}\text{Hg}$ ratios.

Mercury is very volatile and a highly toxic pollutant. Its mobility depends on its different redox states. Reduction of Hg species to $\text{Hg}(0)$ vapor is the most important pathway for removal of Hg from aqueous systems to the atmosphere occurring by biotic and abiotic reactions. Data by Smith et al. (2005), Xie et al. (2005), Foucher and Hintelmann (2006) and Kritee et al. (2007), indicate that mercury isotopes are fractionated in hydrothermal cinnabar ores, sediments and environmental samples. The range in isotope composition ($^{202}\text{Hg}/^{198}\text{Hg}$) is likely to exceed 5‰, quite large considering the relatively small mass range of less than 4%. Smith et al. (2005, 2008) analyzed the Hg isotope composition of fossil hydrothermal systems and concluded that ore and spring deposits have a larger range in Hg isotope composition than